

射頻微機電可調式電感器之設計、模擬與製作

學生：金彥宏

指導教授：羅一中

徐文祥

國立交通大學 機械工程學系 碩士班

摘要

隨著無線通訊產品的進展，如手機、無線區域網路、藍芽傳輸等，都是高頻射頻技術而研發出來的。其中，可以利用射頻微機電技術來製造出輕、薄、短、小的射頻被動元件，它包含了微開關、共振器、高品質電感、可調式電容、可調式電感與可調式濾波器。

本文的重點將集中於可調式電感。研究過程是從選擇電感的調節原理、模擬、製作到最後元件量測。本論文的可調式電感的原理，是利用雙圈雙層電熱式致動器，利用熱膨脹係數不同，而導致線圈會向上或向下彎曲，使得電感值會因為兩個線圈互感值改變而造成總體的電感值變化。本文最後製造出了兩種可調式電感的型式，包含了改變電感的線寬、線圈間的距離、以及利用乾蝕刻與濕蝕刻將基底掏掉。先利用高頻電磁分析軟體 HFSS 來尋求最佳化的設計，希望能達到高品質係數、高的操作頻率、電感值及其改變的範圍能很大，最後在到國家奈米元件實驗室(NDL)去量測高頻結果來驗證。

本文的可調式電感所佔的面積僅有 $540 \mu\text{m} \times 300 \mu\text{m}$ 。量測結果其電感值皆大於 1nH ，而且電感值的調整範圍可以高達 10.4%。藉由將基底掏空，其品質因素可以從 5.35 提升至 16.8。而且其操作頻率可以超過 30GHz，而且在操作頻率 5GHz 時，品質因素最好可到達 16.8。

Design, Simulation, and Fabrication of Tunable RF-MEMS Inductors

Student : Yen-Hong Chin

Advisors : Dr. Yi-Chung Lo

Dr. Wensyang Hsu

Department of Mechanical Engineering

National Chiao Tung University

Abstract

With the wireless communication coming, such as cellular phone、wireless LAN, and Bluetooth, they are developed by RF technology. It will be light、thin、short、and small in order to save the energy and have smaller areaby RF MEMS technology. RF MEMS passive devices include RF micro switch、resonator、high Q inductor、tunable capacitor、tunable inductor, and tunable filter.

This thesis will focus on the tunable inductor. The principle of the tunable inductor is used two-loop thermal bimorph actuators which will be upward or downward because of the different thermal expansion of materials. Two types tunable inductors are fabricated in this thesis, including changing the width, gap, and etching the substrate by dry and wet etching. By using HFSS to optimize the inductor, it will be gotten high Q, high resonant frequency, high inductance and tuning range. At last, we will go to NDL to get the high frequency characteristic to prove the accuracy.

The area of the inductor is only $540\mu\text{m} \times 300\mu\text{m}$. The inductance is all over 1nH. The inductance tuning range is up to 10.4%. The quality factor can be improve from 5.35 to 16.8 after etching $100\mu\text{m}$ deep cavity. The resonant frequency is above 30GHz and the best quality factor is 16.8 at 5GHz.

致謝

本論文的完成，首先要感謝我的指導教授羅一中博士和徐文祥教授。在羅博士的帶領與指導下，讓我有機會接觸到射頻微機電的專業知識，另外在跨領域的學習及待人接物上，使我的視野增廣許多。謝謝徐教授的鼓勵與寬容，在研究所的學習過程中，均不厭其煩的給予我指導與協助，並且提供良好的學習環境，兩位教授不僅在平時的研究討論提供許多寶貴的意見，也帶給我相當多待人處事態度的啟發，使我獲益匪淺。

其次要感謝實驗室的鐘君煒學長、楊涵評學長、蔡梨暖學姐、張駿偉學長、黃家聖學長和李毅家學長的關愛與照顧，對於我在課業上及實驗上的問題，無私的訓練及指導傳授許多製程經驗，使我在實驗初期能很快的上手，並給予我許多的意見及看法，使我獲益良多。

接著也要感謝同屆的實驗室同學：葉昌旗和黃元德，謝謝你們這兩年在碩士生涯的陪伴及實驗製程的討論與協助。

另外也要感謝實驗室學弟：張家維、張耕碩和魏仁宏的關愛及照顧；另外，謝謝趙子元學長在高頻量測方面提供我專業的意見。

最後，我要衷心的感謝我的家人這兩年來生活上的支持及鼓勵，使我在研究所期間能全力以赴，真的很感謝你們的照顧與關心。謝謝。

~僅以本論文，獻給一路上曾幫助我和關心我的人!!~

彥宏 于新竹 • 交大

2006/6/27

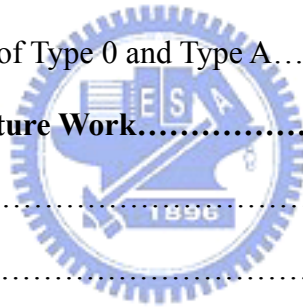
Contents

摘要.....	i
Abstract.....	ii
致謝.....	iii
Contents.....	vi
List of Tables.....	vii
List of Figures.....	viii
Chapter 1 Introduction.....	1
1.1 Introduction.....	1
1.2 Motivation.....	2
1.3 Related Researches.....	3
1.3.1 Extremely High-Q Tunable Inductor for Si-Based RF Integrated circuit applications.....	3
1.3.2 A Micro Variable Inductor Chip Using MEMS Relays.....	4
1.3.3 Self-Assembling MEMS Variable and Fixed RF Inductors.....	4
1.3.4 Fabrication and evaluation of an on-chip micro variable inductor.....	6
1.3.5 A tunable RF MEMS Inductor.....	7
1.3.6 Tunable radio frequency MEMS inductors with thermal bimorph actuators.....	8
1.4 Research Objectives.....	9
1.5 Thesis Organization.....	11
Chapter 2 Inductor Design.....	12
2.1 Introduction.....	12
2.2 Basic Principle.....	12
2.2.1 The Source of the Inductance.....	12

2.2.2 The Series and Parallel Connections of the Inductor.....	15
2.2.3 Self Inductance and Mutual Inductance.....	15
2.3 Equivalent Model.....	17
2.4 Scattering Parameter.....	18
2.5 Insertion Loss and Return Loss.....	19
2.6 Quality Factor.....	20
2.7 Resonant Frequency.....	21
2.8 Skin Effect.....	22
2.9 The Loss of the Inductor.....	23
2.10 Concept Design.....	25
Chapter 3 Inductor Simulation.....	28
3.1 Software Introduction.....	28
3.1.1 Ansoft HFSS.....	28
3.1.2 ANSYS.....	30
3.2 Planar Circuit Design.....	32
3.3 The Effects of Width and the Gap on the Inductors.....	34
3.4 The Effects of the Thickness of the Metal on Inductance and Q.....	36
3.5 The Effects of the Metal Materials on Inductance and Q.....	37
Chapter 4 Fabrication Process.....	39
4.1 Fabrication Flowcharts of Three Types Inductors.....	39
4.2 Substrate Selection and Clean.....	42
4.3 Lithography.....	43
4.4 Reactive Ion Etching.....	43
4.5 Sputtering.....	43
4.6 Electroplating.....	44
4.7 Dry and Wet Etching.....	44



4.8 Fabrication Results.....	45
4.8 Mask Layout.....	46
Chapter 5 Measurement and Results.....	48
5.1 De-embedded Procedure of Measurement.....	48
5.2 On Wafer Measurement.....	49
5.3 Measured Results.....	50
5.3.1 Measured Inductance before Tuning.....	50
5.3.2 Measured Quality Factor before Tuning.....	51
5.3.3 The Inductance Tuning.....	52
5.3.4 The Quality Factor Change with Tuning.....	53
5.3.5 Comparison between Measurements and Simulations.....	55
5.3.6 The Quality Factor of Type 0 and Type A.....	57
Chapter 6 Summary and Future Work.....	58
6.1 Conclusions.....	58
6.2 Future Work.....	59
References.....	60



List of Tables

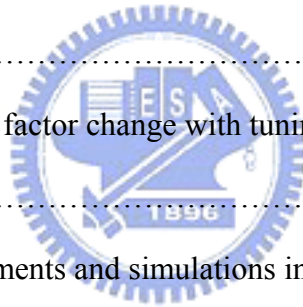
Table 2-1 The skin depth of some materials at 1, 10, 20 GHz.....	23
Table 2-2 The coefficient of thermal expansion.....	26
Table 3-1 The material parameters in ANSYS simulation.....	31
Table 4-1 Fabrication flowcharts of type 0 inductor.....	40
Table 4-2 Fabrication flowcharts of type A inductor.....	40
Table 4-3 Fabrication flowcharts of type B inductor.....	41



List of Figures

Fig. 1.1 (a)the photo of actual tunable inductor (b)measured quality factor (c)measured inductance and resistance [4].....	3
Fig. 1.2 (a)variable inductor circuit diagram (b)a schematic view of microrelay [5]...4	4
Fig. 1.3 Variable self-assembling hairpin inductor [6].....	5
Fig. 1.4 Other types of inductors (a)triangular (b)hinged hairpin (c)meander [6].....	6
Fig. 1.5 The variable inductor of height 200 μm [7].....	7
Fig. 1.6 (a) side view (b) top view of the inductor [8].....	8
Fig. 1.7 Schematic drawing of the tunable inductor [9].....	9
Fig. 2-1 The spiral coil inductor.....	14
Fig. 2-2 The phenomenon of mutual inductance.....	16
Fig. 2-3 The equivalent model of a inductor [10].....	17
Fig. 2-4 Two port network for the incident, a, and reflected, b, waves.....	19
Fig. 2-5 The layout of the tunable inductor and its equivalent model.....	26
Fig. 3-1 The Ansoft HFSS simulation procedures.....	31
Fig. 3-2 The ANSYS simulation in temperature.....	31
Fig. 3-3 The ANSYS simulation in displacement.....	32
Fig. 3-4 The inductor model established by HFSS.....	33
Fig. 3-5 The parameters of the RF tunable inductor.....	33
Fig. 3-6 The inductance and quality factor simulated by HFSS.....	35
Fig. 3-7 The effect of thickness on the inductance.....	36
Fig. 3-8 The effect of thickness on the quality factor.....	37
Fig. 3-9 Effects of Different materials on the simulated inductance and quality factor.....	38
Fig. 4-1 The sketch map of etching substrate (a) only KOH etching(b) XeF2 etching	

first (c) after XeF2 and KOH etching.....	45
Fig. 4-2 The overview of type 0 inductors.....	45
Fig. 4-3 The SEM image of (a) type A G20W10 inductor (b) type A G20W10 inductor and its open circuit.....	46
Fig. 4-4 The mask layout of the tunable inductor.....	47
Fig. 5-1 The sketch of (a) DUT (b) Dummy.....	49
Fig. 5-2 The outline diagram of on-wafer measurement setup with microprobes station and vector network analyzer equipped in NDL RF Lab.....	50
Fig. 5-3 The measured inductance before tuning.....	51
Fig. 5-4 The measured quality factor before tuning.....	51
Fig. 5-5 The measured inductance tuning in (a) G5W10 (b)G10W10 (c) G20W20.....	53
Fig. 5-6 The measured quality factor change with tuning in (a) G5W10 (b) G10W10 (c) G20W20.....	55
Fig. 5-7 Comparison measurements and simulations in (a) inductance and (b) quality factors.....	56
Fig. 5-8 The quality factor of type 0 and type A.....	57



Chapter 1 Introduction

1.1 Introduction

RF, radio frequency, means the electro magnetic wave at high frequency, such as up to 300GHz. Because the velocity of electro magnetic wave is the velocity of the light, the wave length of electro magnetic wave is from 1mm to hundreds km. Ideally, RF and microwave circuits are comprised of interconnections of well-demarcates, including lumped passive elements, such as resistors, capacitors, and inductors, distributed elements, such as microstrip, coplanar waveguide, or rectangular wave guide, and active elements, such as field-effect transistors (FETs) or bipolar transistors.[1]

With the third generation mobile communication coming, the technology of wireless communication is broadly applied in consumer goods, such as cellular phone 、 wireless LAN, and bluetooth. Communication among people and the transmission will not be limited by using wireless mobile communication technology. [2]

In this trend, the production of wireless communication must be RF circuit. It will be light 、 thin 、 short 、 and small in order to save the energy and have smaller area.

Recently, Microelectromechanical System (MEMS) technology in wireless communication is more and more important and it is researched widely. The MEMS applied to RF device is called RF MEMS system. RF device fabricated by traditional semiconductor integrated circuit doesn't have high quality factor. As we know, RF device must have high Q to avoid signal loss, even if the operation frequency is in higher frequency. [2]

There are some advantages in RF MEMS technology. It can be manufactured a lot, in other words, the mask can be used again and again if the pattern doesn't change. Using RF MEMS technology can produce low volume device that can save energy. Furthermore, it can increase the operation frequency to tens of GHz. In addition, RF MEMS device has high integrated ability in IC fabrication. [3]

RF MEMS devices include RF micro switch, resonator, high Q inductor, tunable capacitor, tunable inductor, and tunable filter. The key subject in this thesis is tunable inductor, including tunable range, quality factor, and resonant frequency. [3]

RF inductors are applied in filters, resonators and else. They play an important role in RFIC. In my studies for the papers about RF inductors, most are spiral inductors. Their inductors have high Q and high reliability. It means Q is even greater than 40 and the inductance can be stable no matter how the environment disturb it. In other papers about RF inductors, they are about tunable inductors. They study tunable range, quality factor, and operation frequency. The details will be described in next section.

1.2 Motivation

There is not a general rule to design an inductor. In many papers, the processes of designing the inductor size are not described clearly. In this way, the particular steps in the simulation will be introduced here and presented how to trade off to obtain the final dimensions of the inductor.

There are some ways to make the inductors tunable. The reason for the inductors to be tunable is the distance between coil and coil to be changed. In this way, they can be seen as micro-actuators. Micro-actuator includes five primary

types, such as static electricity 、 electro-thermal 、 electro-magnetic 、 piezoelectricity, and gas/liquid actuate micro-actuators [3]. In this paper, electro-thermal actuator is chosen to be a tunable inductor.

1.3 Related Researches

1.3.1 Extremely High-Q Tunable Inductor for Si-Based RF Integrated circuit applications [4]

In 1997, Pehlke describe a high Q tunable inductor. He used two inductors, and one of them can be shifted by phase to influence the mutual inductance. The tuning range of the inductance is over 100% as shown in Fig.1.1. Q is up to 2000 at 2GHz.

This paper is the first one about the tunable inductor. Although the quality factor and tuning range is very high, the operating frequency in this paper is only 2 GHz. It seems too small. Besides, a couple of tunable inductors need two inductors, one as RF inductor and the other as drive inductor which is shifted the phase of AC current. The power input is twice of other types of tunable inductors. The drive inductor is also probably jamming other inductor if there are other inductors.

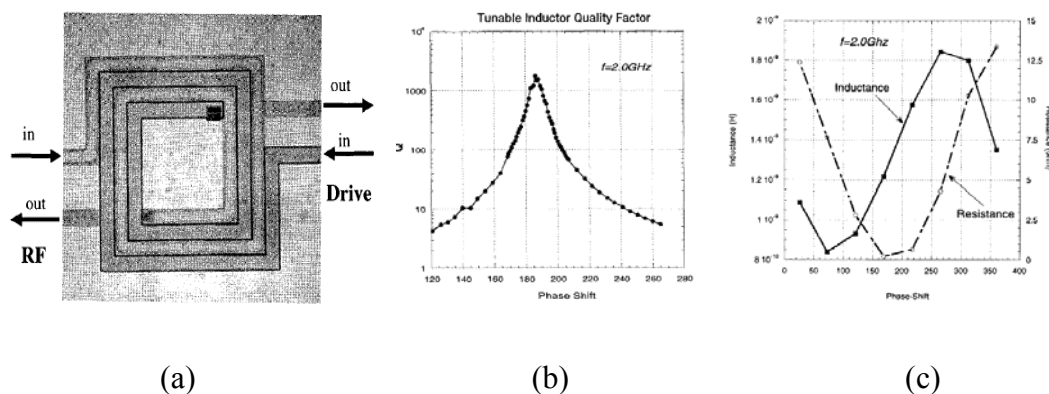


Fig. 1.1 (a) the photo of actual tunable inductor (b)measured quality factor (c)measured inductance and resistance [4]

1.3.2 A Micro Variable Inductor Chip Using MEMS Relays [5]

In 1997, Zhou developed an adjustable inductor controlled by microrelays which were fabricated with a $\text{TaSi}_2/\text{SiO}_2$ bimorph cantilever beam, combined electrostatic and thermal actuation mechanism, as shown in Fig1.2(a). By using four microrelays, sixteen different inductance will be produced from 2.5 nH to 324.8 nH. The inductors is a 16-turn rectangular spiral shape, and the value of L_3 , L_2 , L_1 and L_0 are 77 nH, 42nH, 29nH and 15 nH.

The advantage of this type inductor is the high variable range. If there is more inductors and microrelays, the range will be higher. But there are still some disadvantages. First, it is not “an” inductor but a couple of inductors. The fabrication process used seven photomasks, so it is very complex. The quality factor in this paper isn't mentioned so that the Q can not be understood. The operating frequency is only from 500 MHz to 1.6 GHz.

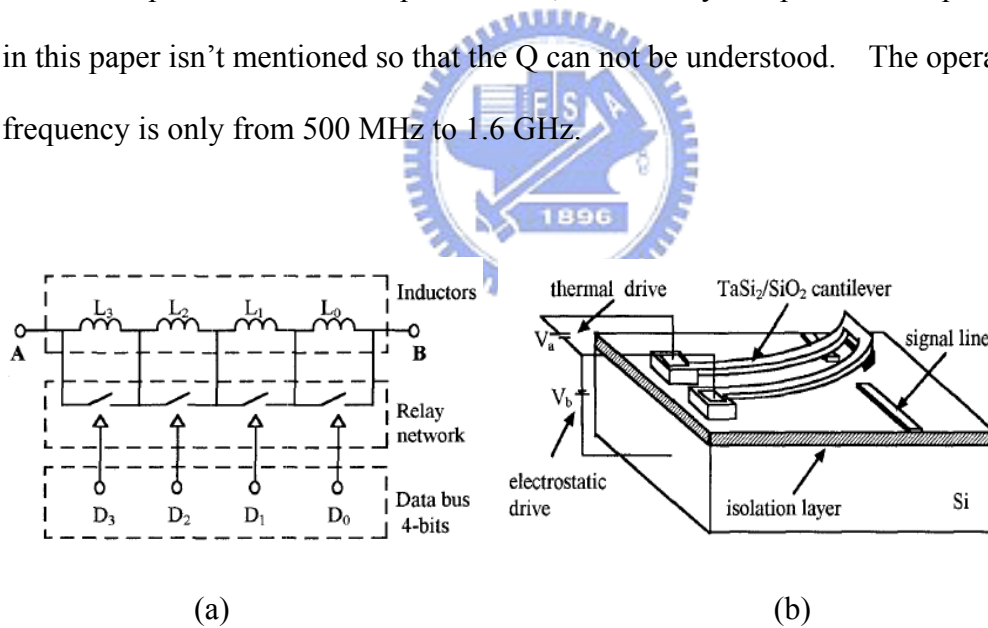


Fig. 1.2 (a) variable inductor circuit diagram (b) a schematic view of microrelay [5]

1.3.3 Self-Assembling MEMS Variable and Fixed RF Inductors [6]

In 2001, Lubecke developed that which can be fabricated on conventional RFIC silicon substrate, which use warping members to assemble themselves away from the substrate to improve the quality factor and self-resonant frequency. The inductor

structure in this paper illustrates as Figure 1.3.

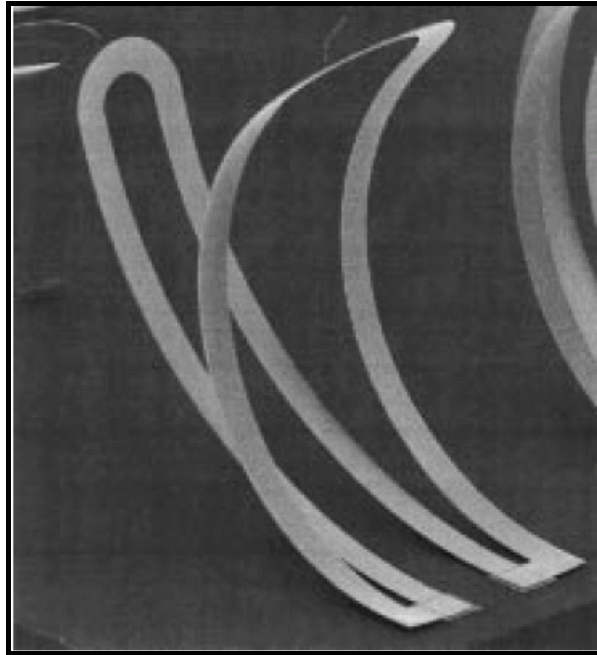


Fig. 1.3 Variable self-assembling hairpin inductor [6]

In order to reduce the parasitic capacitance for high Q, he use two or more material layers deposited with different stresses. The inductor can be made to curl away from the substrate when the sacrificial layer is removed.

When the temperature is heated from 25°C to 200°C, the effect of thermal deformation will be changed. In this case, the Q remained stable around 5, the inductance varied from 0.67 to 0.82 nH (about 18%). There are some other types geometry of self-assembling inductors, as shown in figure 1.4.

The detail size of hairpin shape inductor is 1160µm long, the gap of inner and outer loop 5 to 25µm, 30µm width, and the pitch of anchor pad is 100µm.

The Q can be above 13 (even greater than 20 with additional metal) . Most inductors can be operated up to 20GHz. The inductance is about 1nH and the tuning range is 18% (even up to 30% by optimal structures) .

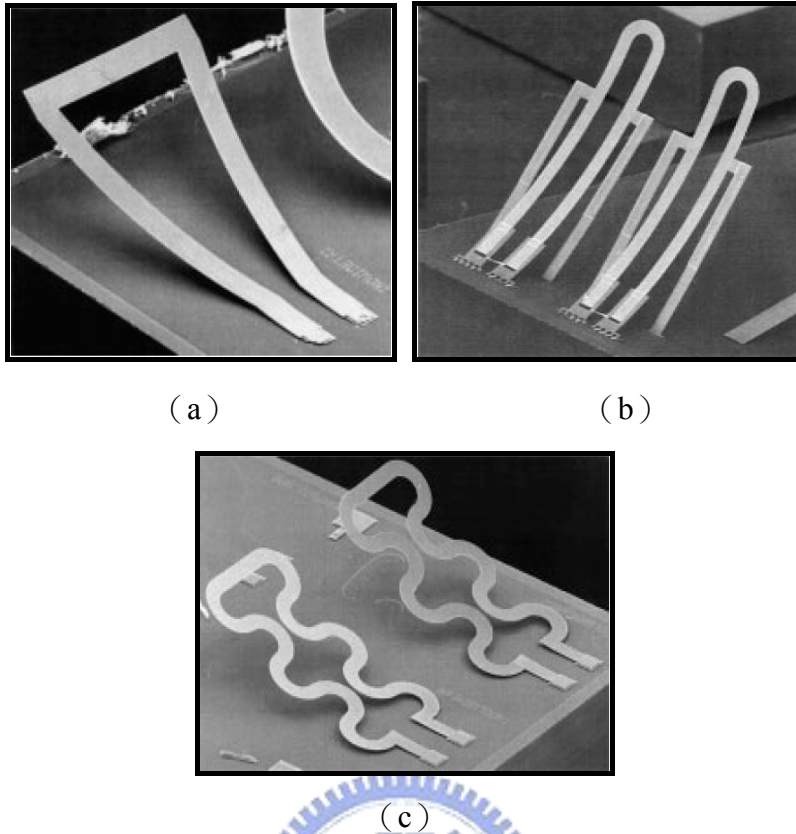


Fig. 1.4 Other types of inductors (a) triangular (b) hinged hairpin (c) meander [6]

1.3.4 Fabrication and evaluation of an on-chip micro variable inductor [7]

In 2003, Fukushige used a new MEMS material, thin film metallic glass (TFMG) . When the temperature is increased, the TFMG will be soften. In the same time, the structure will be lifted up, as shown in Fig. 1.5 .

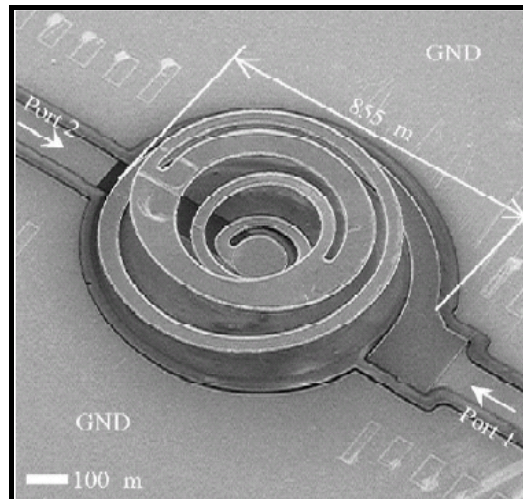


Fig. 1.5 The variable inductor of height 200 μm [7]

The characteristic of this paper is Fukushima using a special material which would be softened in high temperature and would be hardened when the temperature was cooled down. When TFMG was softened, it would be lifted up by using a 3D Micro Manipulator.

The coil height can be changed from zero to several hundred micrometers. The operating frequency can be up to 16 GHz. The inductance tunable range is from 3.64 to 3.75 nH at 2GHz (about 3%). The quality factor is only 2 because of the material TFMG with high resistivity.

1.3.5 A tunable RF MEMS Inductor [8]

In 2004, Abidine reported a single-wafer micromachined RF inductor that can be integrated in a conventional RFIC device. The inductors are made of two different thermal expansion coefficients, such as silicon nitride and gold, forming a thermal bimorph, as shown in Fig 1.6. The outer loop of the inductor is connected by silicon nitride to hold its position without moving. When a current is through the inductor, it caused the inner loop to move downward because of the different thermal

coefficient.

The silicon nitride is $0.6\mu\text{m}$, and the gold is $1\mu\text{m}$ with the $0.1\mu\text{m}$ chrome as an adhesion layer. At last, the inductor will be dug a $300\mu\text{m}$ cavity by using KOH anisotropic etch. The paper used Ansys to simulate the tip deflection versus temperature. The deflection is from $20\mu\text{m}$ to $320\mu\text{m}$ when the temperature is from 300K to 700K.

The inductor has a 8% tuning range and can be operated above 15 GHz. The quality factor is greater than 9 at 5GHz.

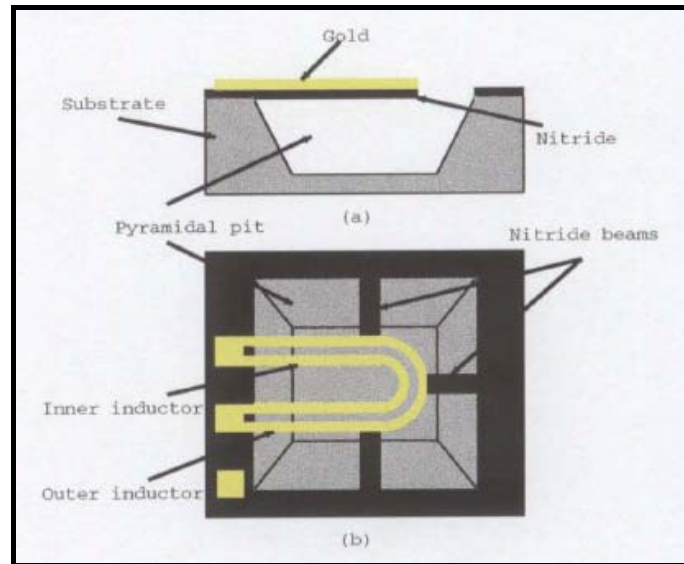


Fig. 1.6 (a) side view (b) top view of the inductor[8]

1.3.6 Tunable radio frequency MEMS inductors with thermal bimorph actuators

[9]

In 2005, Imed used two additional thermal actuators at both sides of outer loop instead of heating the inductor to make it move, as shown in Fig. 1.7. He also designed three different size inductors in order to show the trade-offs of the design. In this research, the tuning range of inductance is about 30%. The best quality factor can be up to 25. The self-resonant frequency of all the inductors is over 35 GHz.

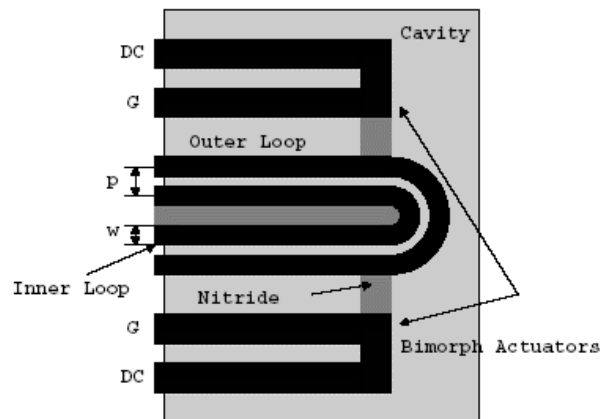


Fig. 1.7 Schematic drawing of the tunable inductor [9]

1.4 Research Objectives

An inductor plays a key role in the RF device, especially a tunable inductor. For example, wide range tuning is necessary in cell phones. On the other hand, narrow range tuning also should not to be neglected. Both of them are important. [6]

The investigation of most papers have few discussion about how to improve the tunable range, over 10% better, and the inductance can be above 1nH. The measurement of inductance will be much more error if the inductance is too small. There are many ways to make the inductance variable. The direct idea is to make the distance of each circuit change. In this way, the inductance will be tuned because of the change of the mutual inductance. In terms of the mechanism, a thermal bimorph is the easiest way to manufacture a cantilever beam. Although its response is slower than other actuator, its deflection is the best. It is considered that the inductor using bimorph type can be the high tuning range.

Because of the precise displacement in electrostatic actuator, the inductor might be added two electrostatic actuators to make outer loop displacement as precise as possible.

The quality factor is also important because it can prevent the signal from losing too much. Many researchers, quality factor of a tunable inductor is not satisfied, only 2 or 9, and the best is 13.

By using Ansoft HFSS and ANSYS, the high frequency electro-magnetic and electro-thermal simulation tools, a high tuning range and Q inductor will be designed, choosing MEMS to fabricate, digging the Si substrate to raise the Q. The influence of materials and size is considered or can fabricate it and justify the simulation and measurement.

Last, using E8364B Network Analyzer can get the result of the high frequency characteristic, inductance and quality factor. After that, the result of tunable inductor will be obtained. At the same time, the high Q and tuning range inductor will be generated.

In short, the main research objectives can be listed in several items as follows:

1. The inductance tuning range must be greater than 10%.
2. The inductance has to above 1 nH to reduce the measurement error.
3. The quality factor is not smaller than 10.
4. The self-resonant frequency is 15GHz at least.
5. The full size of the inductor is less than $1\text{mm} \times 1\text{mm}$.

1.5 Thesis Organization

The thesis includes six chapters. In chapter 1, motivation, related researches, and research objective are described. In chapter 2, the basic principle and design of the tunable inductance are presented. The simulations of Ansoft HFSS and ANSYS are introduced, and the simulation result will be discussed in chapter 3. In chapter 4, the fabrication processes and results of tunable inductors are presented. High frequency measurement setup and measurement are shown in chapter 5. Last, some discussions and conclusions are made up in chapter 6.



Chapter 2 Inductor Design

2.1 Introduction

RF MEMS tunable inductors provide some advantages like the miniaturizing and the tunable inductance. The inductors in RF passive devices are applied in filters, resonators and else. They are playing an important role in RFIC.

In this chapter, there are a lot of characteristics to be discussed in tunable inductors, such as the principle of inductor, its equivalent model, loss, quality factor, resonant frequency, inductance tuning range....., etc. Finally, the conceptual design of tunable inductor will be described.

2.2 Basic Principle

2.2.1 The Source of the Inductance

Most inductors are made of metal conducting wires. When the wires are made to coil, they will be inductors. When the current pass through the coil, it will produce the magnetic field. The magnetic line of force pass through the magnetic field is called magnetic flux, represented by the symbol Φ , and its unit is Weber (Wb). In a unit area, the magnetic flux passed through is defined as magnetic flux density, represented as the symbol B , as shown as equation 2-1 :

$$B = \frac{\Phi}{A} \quad (2-1)$$

where A is the section area, and the unit of the magnetic flux density is Gauss in CGS system or Tesla (Wb/m^2) in MKS system.

Some materials, such as the iron, are easier produced the magnetic flux than other materials, such as air. The permeability of the material is defined to compare the ability of producing the magnetic flux, represented as the symbol μ . The

permeability in vacuum is μ_0 , and the value is $4\pi \times 10^{-7} \text{ Wb} / \text{A} \cdot \text{m}$. The relative permeability μ_r , is the ratio of the permeability of the material to μ_0 . The other permeability of the material is μ , as the equation 2-2 :

$$\mu = \mu_r \times \mu_0 \quad (2-2)$$

In 1831, Faraday found that the changing of magnetic flux will produce a reaction voltage from beginning to end in the coil, as known as Faraday's Law, as the equation 2-3 :

$$V = N \frac{d\Phi}{dt} \quad (2-3)$$

where V is the reaction voltage, $\frac{d\Phi}{dt}$ is the differential of magnetic flux on time.

So there is only the reactive voltage generated when the magnetic flux exist and has variation. The polarity of the reaction voltage is attempting a current to resist the variation of the magnetic flux as the Lenz's Law.

According to equation 2-3, the equation 2-4 will be gotten :

$$V = -N \frac{d\Phi}{dt} = -N \frac{d\Phi}{di} \cdot \frac{di}{dt} = -L \frac{di}{dt} \quad (2-4)$$

The inductance will be defined as equation 2-5 :

$$L = N \frac{d\Phi}{di} \quad (2-5)$$

The unit of the inductance is Henry (H). In RF MEMS inductor, nano Henry (nH) is the most useful unit.

If there is a N turns spiral coil, around a section area $A \text{ m}^2$, the length of the coil is l, and the permeability of the material is μ , as shown in Fig. 2-1.

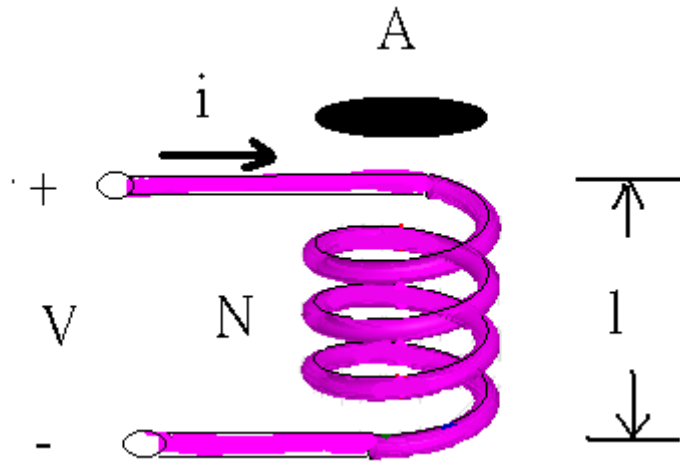


Fig. 2-1 The spiral coil inductor

According to the Ampere's Law,

$$N \cdot i = H \cdot l + H_a \cdot l_a \quad (2-6)$$

$H_a \cdot l_a$ is ignored, the equation will be

$$\begin{aligned} N \cdot i &= H \cdot l \\ &= \frac{Bl}{\mu_0} = \frac{\Phi l}{\mu_0 A} \end{aligned} \quad (2-7)$$

Let the reluctance R is $\frac{1}{\mu_0 A}$

$$N \cdot i = \Phi \cdot R \quad (2-8)$$

$$\therefore \Phi = \frac{N \cdot i}{R} = \frac{H \cdot i \cdot \mu \cdot A}{l} \quad (2-9)$$

By the equation 2-5 and 2-9, the inductance L will be equation 2-10

$$L = \frac{\mu \cdot N^2 \cdot A}{l} \quad (2-10)$$

From the equation 2-10, there are some parameters in the spiral inductors :

- (a) The turns of the coil. The inductance is a direct ratio to the square of the turns.
- (b) The section area of the coil center. The inductance will increase while the area is increasing.
- (c) The length of the coil. The inductance is an inverse ratio to the length of the coil.

(d) The permeability of the coil material. The inductance will increase while the permeability of the coil material is increasing.

2.2.2 The Series and Parallel Connections of the Inductor

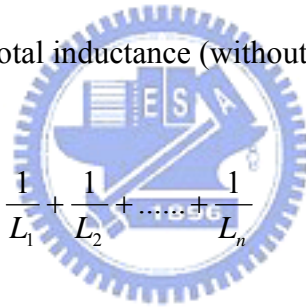
In the circuit, the inductor can be combination as the resist, such as series and parallel connection.

According to equation 2-4, the inductance is a direct ratio to the voltage. From Ohm's Law, the voltage in the resist is a direct ratio to resist. Thus it can be seen that the situation of inductors and resists is the same. The total inductance is the sum of each inductance (without considering mutual inductance), as the equation 2-11 :

$$L_t = L_1 + L_2 + L_3 + \dots + L_n \quad (2-11)$$

As the same reason, the total inductance (without considering mutual inductance) in the parallel connection is :

$$\frac{1}{L_t} = \frac{1}{L_1} + \frac{1}{L_2} + \dots + \frac{1}{L_n} \quad (2-12)$$



2.2.3 Self Inductance and Mutual Inductance

If the coil is more than two loops, the inductance has not only self-inductance but also mutual-inductance. It can be known that the inductance is the direct ratio to the magnetic flux from equation 2-5. As the result, the total inductance is the self-inductance plus mutual inductance.

The total inductance in inductors is including two types, self inductance and mutual inductance. When the current is passing through the coil changes, the magnetic flux in the coil will change. According equation (2-4), the current in the coil will response a induction electromotive force (EMF). The symbol L in equation 2-4 is the self inductance.

If there are two coils are placed together such as Fig. 2-2, when a current i_1 is into the coil 1, there are the magnetic fluxes generated, $\Phi_1 = \Phi_{11} + \Phi_{12}$. Φ_{11} is call the magnetic loss and Φ_{12} is called the mutual magnetic. In the other hand, there will be $\Phi_2 = \Phi_{22} + \Phi_{21}$ in the coil 2. Thus, the mutual induction EMF in the coil 2 is:

$$\begin{aligned} V_{21} &= -N_2 \frac{d\Phi_{12}}{dt} = -N_2 \frac{d\Phi_{12}}{di_1} \cdot \frac{di_1}{dt} \\ &= -\frac{N_2 \Phi_{12}}{i_1} \cdot \frac{di_1}{dt} = -M_{21} \cdot \frac{di_1}{dt} \end{aligned} \quad (2-13)$$

$$\therefore M_{21} = \frac{N_2 \Phi_{12}}{i_1}$$

M_{21} is the mutual inductance which is the coil1 to the coil 2.

As the same reason, the mutual inductance M_{12} is :

$$M_{12} = \frac{N_1 \Phi_{21}}{i_2}$$

In this case, the total inductance of coil 1 is $L_1 + M_{12}$.

$$\begin{aligned} L_{1_total} &= L_1 + M_{12} \\ &= N \frac{d\Phi}{di} + \frac{N_1 \Phi_{21}}{i_2} \end{aligned} \quad (2-14)$$

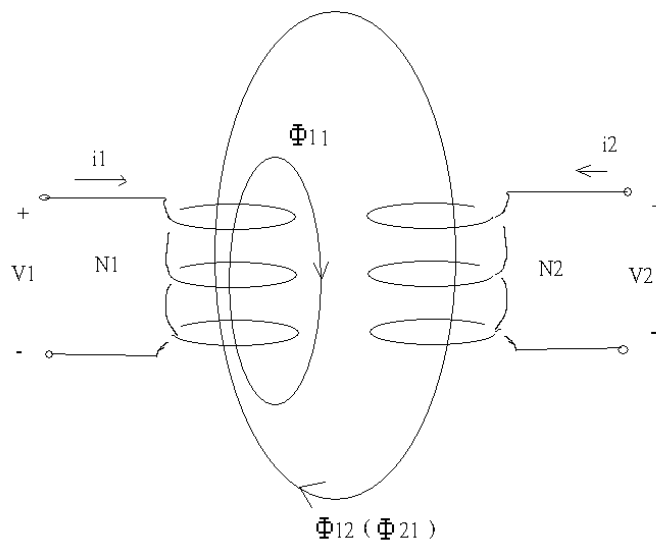


Fig. 2-2 The phenomenon of mutual inductance

2.3 Equivalent Model

The performance of a planar inductor needs to be understood when designing a inductor. Thus, the LRC equivalent model is described in Fig. 2-3 [10].

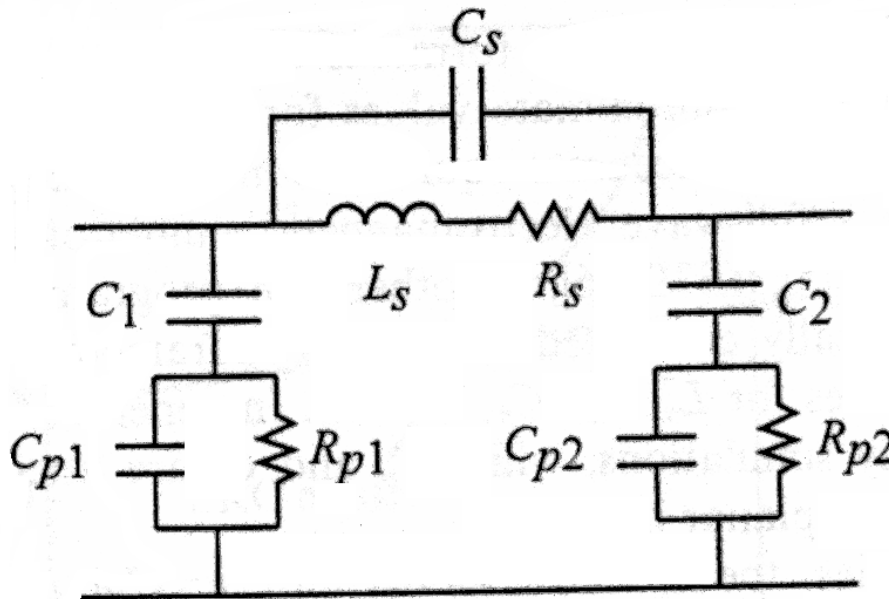


Fig. 2-3 The equivalent model of a inductor [10]

L_s is the inductance in low frequency. The value is based on the loops of the coil.

R_s is the series resistance of the coil. The value is the primarily factor of the quality factor in low frequency. It affects the resonant frequency directly.

C_s is the capacitance which is generated by different coils and by air and the dielectric layers. In the low frequency, it is the same potential between the coil and the coil.

As the result, C_s can be neglected. In high frequency, the parasitism capacitance effect is more obvious, but it can be reduced by adding the gap of coils.

C_1 is the capacitance which is between silicon and the coil in the oxide (or polyamide) layer.

C_p is the capacitance between the coil and the ground through the silicon substrate.

R_p is the eddy current losses in the substrate.

At low frequency, the model of the inductor in Fig. 2-3 will become an L_s , R_s model, and the input impedance of the inductor will be the equation 2-15 :

$$Z = R_s + j\omega L_s \quad (2-15)$$

The inductance will become the equation 2-16 :

$$\Rightarrow L = \frac{Z}{j\omega} = -\frac{jZ}{\omega} = -\frac{1}{2\pi \cdot f \cdot \text{Im}(Y)} \quad (2-16)$$

At high frequency, the capacitance can not be neglected. Assume one side of the inductor is connected to the ground, and C_1 and C_{p1} are lumped together in one capacitance, C_p . The input impedance will be equation 2-17 :

$$Z = (R_s + j\omega L_s) \left\| \left(\frac{1}{\omega C_s} \right) \left\| \left(\frac{1}{\omega C_p} + \left(\frac{1}{\omega C_p} \right) \parallel R_{p1} \right) \right\| \right\} \quad (2-17)$$

2.4 Scattering Parameter

Because the requirements of short- and open-circuit terminations are not become easily for evaluation at high frequency, the general Z , Y parameters are not suitable to describe the high frequency circuit. The S parameters are particularly desirable because their evaluation does not require short- or open-circuit terminations [11].

The scattering or S -parameter can describe the characteristic in two-port network.

The signals of electro magnetic wave energy in two-port network are divided into transmission and reflection, and their concepts are shown in Fig. 2-4. The incident waves are represented as a_i and the reflect waves are represented as b_i , where i is the number of the port. The characteristic of the transmission line can be obtained by the transmission/reflection ratio, so called S -parameter.

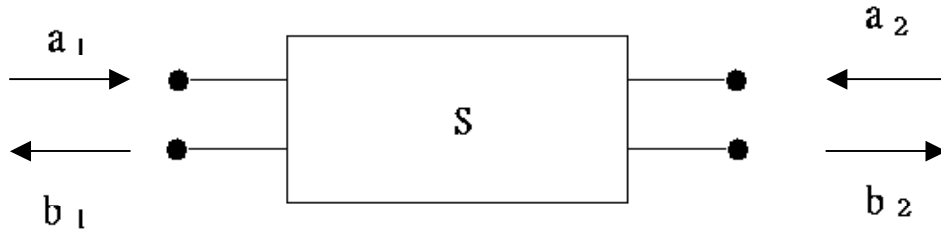


Fig. 2-4 Two port network for the incident, a, and reflected, b, waves

Based on Fig. 2-4, for the two-port network, the b wave leaving port 1 is the phase sum of a wave reflected from the input port ($S_{11}a_1$) plus a wave that passed through the two-port from port 2 ($S_{12}a_2$) :

$$b_1 = S_{11}a_1 + S_{12}a_2 \quad (2-18)$$

Similarly

$$b_2 = S_{21}a_1 + S_{22}a_2$$

The individual S parameters are evaluated using these relationships :

$$\begin{aligned}
 S_{11} &= \left. \frac{b_1}{a_1} \right|_{a_2 = 0} \\
 S_{12} &= \left. \frac{b_1}{a_2} \right|_{a_1 = 0} \\
 S_{21} &= \left. \frac{b_2}{a_1} \right|_{a_2 = 0} \\
 S_{22} &= \left. \frac{b_2}{a_2} \right|_{a_1 = 0}
 \end{aligned} \quad (2-19)$$

2.5 Insertion Loss and Return Loss

When a transmission line which its impedance is Z_0 connects with a transmission line whose impedance is Z_L , some electro magnetic wave energy will be reflect, and most of it will transfer to the load Z_L . The amplitude of vibration for Z_L can be defined by transmission coefficient, such as equation 2-20 :

$$T = 1 + \Gamma = 1 + \frac{Z_L - Z_0}{Z_L + Z_0} = \frac{2Z_L}{Z_L + Z_0} \quad (2-20)$$

There is no energy loss in ideal electro magnetic wave energy transmission, but there will be energy loss in real situation. The insertion loss (IL) is defined as the equation 2-21, which is usually represented by S_{21} .

$$IL = -20 \log |T| \quad (2-21)$$

The electro magnetic wave energy can not be all transferred to the load if two transmission lines are not matched. There will be energy loss at signal input, and this kind of energy loss is defined as return loss, such as equation 2-22, which is usually represented by S_{11} .

$$RL = 20 \log |\Gamma| \quad (2-22)$$

2.6 Quality Factor

Radio frequency and microwave circuit process information-carrying signals characterized by an incoming power level and a frequency spectrum. There is a parameter describing the selectivity of the inductor, as known as the quality factor, which defined the ratio of the maximum instantaneous energy stored in the circuit to the energy loss per cycle [12], as shown in equation 2-23 :

$$Q = 2\pi \times \frac{\text{maximum instantaneous energy stored in the circuit}}{\text{energy dissipated per cycle}} \quad (2-23)$$

It is customary to consider the power loss as consisting of the power loss associate with the external load and the inductor itself. The resulting quality factor is named loaded Q or measured Q, and the Q_L can be cast in the form in as follows [13] :

$$Q_L = \frac{f_c}{BW^{3dB}} \quad (2-24)$$

Where f_c is the resonance frequency and BW^{3dB} is the bandwidth, which is defined as the difference between upper and lower frequencies recorded at the 3 dB attenuation points above the passband.

The primarily energy of ideal inductor is saved as the magnetic energy generated by the magnetic field, some saved as the electro energy generated by the electro field because of the parasitic capacitance. In an inductor, the quality factor is the ratio of its reactance magnitude to its resistance as shown as equation 2-25 :

$$Q = \frac{\text{reactance}}{\text{resistance}} = \frac{X_L}{R_L} = \frac{\omega L}{R_L} \quad (2-25)$$

Based on equation 2-25, the quality factor can be written as equation 2-26 :

$$Q = \frac{\text{Im}(Z)}{\text{Re}(Z)} = -\frac{\text{Im}(Y)}{\text{Re}(Y)} \quad (2-26)$$

where Y is the admittance which is the complex reciprocal of impedance Z.

2.7 Resonant Frequency

The impedance constructed by RLC circuit is the function of frequency. The impedance is divided of resistance in real part and the reactance in image part. At some frequency, the reactance will be zero so that the impedance is only including resistance. This phenomenon is called resonance, and the frequency will be called resonant frequency at this frequency.

In the RF inductor, it has two characteristics, inductor and capacitor. Below the resonant frequency, the inductor characteristic is priority in capacitor. On the other hand, the inductor will become capacitor characteristic at the frequency that is upper the resonant frequency.

The parasitic capacitance in the substrate is the dominant capacitance for medium to large value inductors, and the inductor resonant frequency is given using the circuit of Fig. 2-3 : [10]

$$f_r = \frac{1}{2\pi\sqrt{L_s \cdot C_p}} \quad (2-27)$$

In general, $C_s \ll C_p$ and is neglected in the resonant frequency calculation. However, for micromachined inductors with a very low parasitic capacitance and a high resonant frequency, it must include C_s in the circuit model. In this case, the resonant frequency will become equation 2-28 :

$$f_r = \frac{1}{2\pi\sqrt{L_s(C_p + C_s)}} \quad (2-28)$$

2.8 Skin Effect

In DC or low frequency circuit, the electron of the current in a conducting wire is spread averagely on the cross area of the conducting wire. When the frequency is higher, the electron current will be from the center of the wire to the edge so that the current will concentrate the surface of the wire. It is called skin effect that the focus of the current will add the resistance. In this case, the resistance per unit length is given by equation 2-29 :

$$R_s = \frac{\rho}{\delta w} \quad (2-29)$$

Where ρ (Ω -cm) is the metal resistivity, w is the width of the conduction wire, and the δ is the skin depth defined as the distance it takes the field to decay exponentially to $e^{-1} = 0.368$, or 36.8% of its value at the air-conductor interface, such as equation 2-30 :

$$\delta = \sqrt{\frac{\rho}{\pi\mu f}} \quad (2-30)$$

Where μ is $4\pi \times 10^{-7} H/m$, and f is the operation frequency. In general, the metal thickness must twice to skin depth to obtain as low RF resistance as possibly. The

resistivity and the skin depth in then frequency from 1 GHz to 20 GHz of some metals will be shown in Table 2-1 :

Table 2-1 The skin depth of some materials at 1, 10, 20 GHz

	$\rho(\Omega\text{-cm})$ [9]	δ at 1 GHz	δ at 10 GHz	δ at 20 GHz
Cu	1.67×10^{-6}	2.06 μm	0.65 μm	0.16 μm
Au	2.35×10^{-6}	2.44 μm	0.77 μm	0.19 μm
Al	2.65×10^{-6}	2.60 μm	0.82 μm	0.21 μm
Ti	42×10^{-6}	10.31 μm	3.26 μm	0.82 μm

2.9 The Loss of the Inductor

In a RF inductor, the quality factor is the most concerned, and the magnitude of the quality factor is related with the energy of inductor stored, as shown in section 2-6. It is necessary to realize the inductor loss. In low frequency, the primary loss is from the metal skin effect ; in high frequency, the loss is primary from the substrate loss because the impedance of the substrate shrinks so that the signal will loss easily from the substrate. The factors of the inductor loss are including metal loss and substrate loss.

A. Metal Loss

The series resistance can be calculated easily from the sheet resistance in low frequency as shown in equation 2-31 :

$$R_s = R_{sheet} \cdot \frac{l}{w} \quad (2-31)$$

Where l is the total length and w is the width of the resist.

In high frequency, because of the skin effect, as shown in section 2-8, it will cause the current unequally and add the loss of the metal.

Therefore, in designing the inductor, there should not be any circuit in the center of the inductor where the magnetic field is bigger in order to avoid increasing the series resistance because the current is concentrated too much. In the cause of decreasing the energy loss of the inductor on the metal, it can be added the width and the thickness to raise the cross section so that the resistance will be decrease. But it will increase the parasitic capacitance so that the resonant frequency will decrease.

B. Substrate Loss

The Si substrate will be generated eddy current by changing the inductor magnetic field. It will cause the additional resistance loss and reduce the inductance. Besides, the capacitance between the metal and the substrate will couple the current in the substrate to the metal and bring the noise from the substrate to the metal.

C. Radiation Loss

There is always the radiation loss while the energy of the electro magnetic wave transports in the transmission lines. The radiation loss is related to the dielectric constant, the thickness of the substrate, and the structure of the transmission line. Not considering the structure, the radiation resist R_r can be shown in equation 2-32 :

$$R_r = 80\pi^2 \left(\frac{h}{\lambda_0} \right)^2 \quad (2-32)$$

Where h is the length of the metal and the λ_0 is the wave length in free space. [11]

In actually transmission line, the radiation resist will smaller than the impedance of the transmission line. The radiation loss will reduce when the impedance is

increasing.

The shape of the inductor is also related to the loss of the inductor. There will be radiation loss easily if the corner is too sharp. It must be paid attention to the shape when designing a inductor.

2.10 Concept Design

The tunable inductor in this thesis is used thermal bimorph method to make the mutual inductance a change. While the mutual inductance can be changed, the inductor will be tunable, as shown in section 2.2.3. The inductor is two loops as section 1.2.5, but the materials, size, goals, and performance will not be same with that.

The principle of thermal bimorph is using by the difference coefficient of thermal expansion (ppm/K). The structure can be seen as a resist. While the current passes through it, the structure, such as a cantilever beam in this thesis inductor, the temperature will grow up. There will be a linear thermal expansion in this structure. The value of the thermal expansion ΔL is shown in equation 2-33 :

$$\Delta L = \alpha \cdot L \cdot \Delta T \quad (2-23)$$

Where L is the length of the structure, α is the coefficient of the linear thermal expansion, and the ΔT is the value of the temperature raising by inputting the current to control it.

With the different coefficient thermal expansion of two (or more than two) materials, the actuator will be out of plane result from the different thermal expansion of different materials. There are some coefficients of thermal expansion with materials which might be used in this thesis in Table 2-2 [10] :

Table 2-2 The coefficient of thermal expansion

Material	Si ₃ N ₄	Cr	Ti	Au	Cu	Al
α	1.6	4.9~8.2	8.6	14.2	16.5	23.1

The substrate is Si, and Si₃N₄ is the isolation layer and one of the structures. In order to increase self resonant frequency and quality factor, the substrate will be removed by KOH etching. Fig. 2-5 is shown the layout of the tunable inductor and its equivalent model.

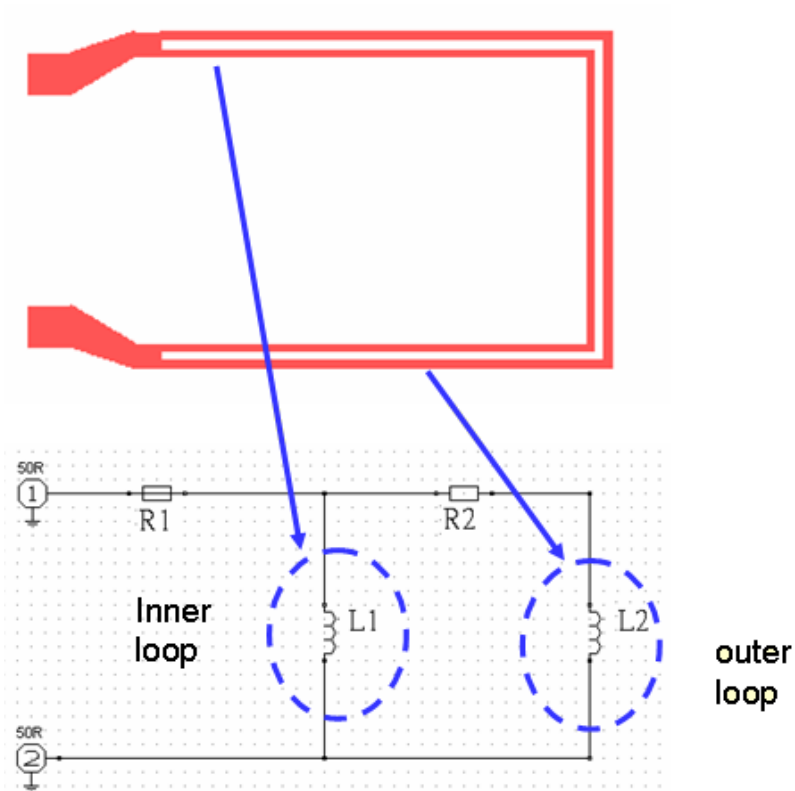


Fig. 2-5 The layout of the tunable inductor and its equivalent model

There are two loops in this inductor, inner loop and outer loop can be seen as parallel connection. The total inductance is $L1+L2+M12$, where $M12$ is the mutual inductance. While the temperature is growing up, the outer loop and inner loop will

be winding because of the difference of the thermal expansion. Therefore, the inductance will be tunable.

There are three primary designs of tunable inductors in this thesis :

Type 0

The purpose of this type of inductors is to be a contrast the quality factor between type A. Theoretically, it will gain the quality factor if the inductor is removed from the substrate. This type inductors will not etch a cave by KOH but the others will.

Type A

The structure layers of the inductor are silicon nitride and copper. At the same time, there are silicon nitride beams at the outside to prevent the outer loop upward or downward.

Type B

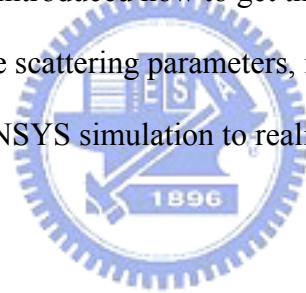
There are still silicon nitride beams at the outside to prevent the outer loop upward or downward. However, the structure layers are some metal materials and copper. The metal materials here are indicated as Al, Cr, or Ti.

The detail fabrication process will be mentioned in chapter 4.

Chapter 3 Inductor Simulation

In communication systems, the operating frequency of the microwave circuit is among 300MHz to 300GHz, and the wave length of the electro magnetic wave is very small so that the energy is also strong. Therefore many high frequency characteristics will affect the operating of the circuit, such as dispersion effect, skin effect, stray effect. In addition, the values equivalent resistance, inductance, and capacitance are not fixed as the frequency is changing. It is a difficult work to solve electro magnetic field. For this reason, a computer assisted design tool, the EM (electro-magnetic) simulation, will be used to predict the characteristics of the inductors. [15]

In this chapter, it will be introduced how to get the result in the high frequency simulation tool, HFSS, and the scattering parameters, inductors, quality factor will be determined. There is also ANSYS simulation to realize the bimorph actuator and its mechanical characteristics.



3.1 Software Introduction

3.1.1 Ansoft HFSS

HFSS, called “High Frequency Structure Simulation”, is a three dimension tool used finite element method (FEM) to simulate full wave electro magnetic by meshing the microwave circuit as finite small meshes. It can be used to calculate parameters such as S-parameter, resonant frequency, inductance, and quality factor. Generally, it can be applied to an antenna, filter, transmission line, and an inductor. It can also predict the high frequency characteristic precisely in microwave circuit, such as the parasitic inductance and capacitance considered to calculate.

The simulation processes are as shown in Fig. 3-1, and the detail setup and the procedures will be described step by step as follows ;

1. Choose the solution type : In this research, the driven terminal will be select to simulate the inductance.
2. Setup the unit and material property : It is more convenient to set the unit be micro meter, and the properties of the material in the inductor must be defined.
3. Drawing the circuit structure : Using the pre-processor to draw the structure and geometry of the inductor, at the same time, the thickness of air box must be five to ten times thicker than the one of the substrate. If thickness of the air box is insufficient, the software might generate errors due to the omitted electromagnetic waves. [13]
4. Assigning boundary condition, wave port, and mesh operations : Define the vectors of the input and output port. Define the perfect conductor and radiation faces. Last, assign the number of mesh element is 5000.
5. Setup the analysis and solution parameters : In this research, delta S is defined 0.005 as the convergence condition. The target of Lambda refinement is 0.05 to help consider the effects of high frequency.
6. Start to solving and view the result : After solving finished, the results, for example, inductance and quality factor will be obtained by formula, as shown as equation 2-16 and 2-26.

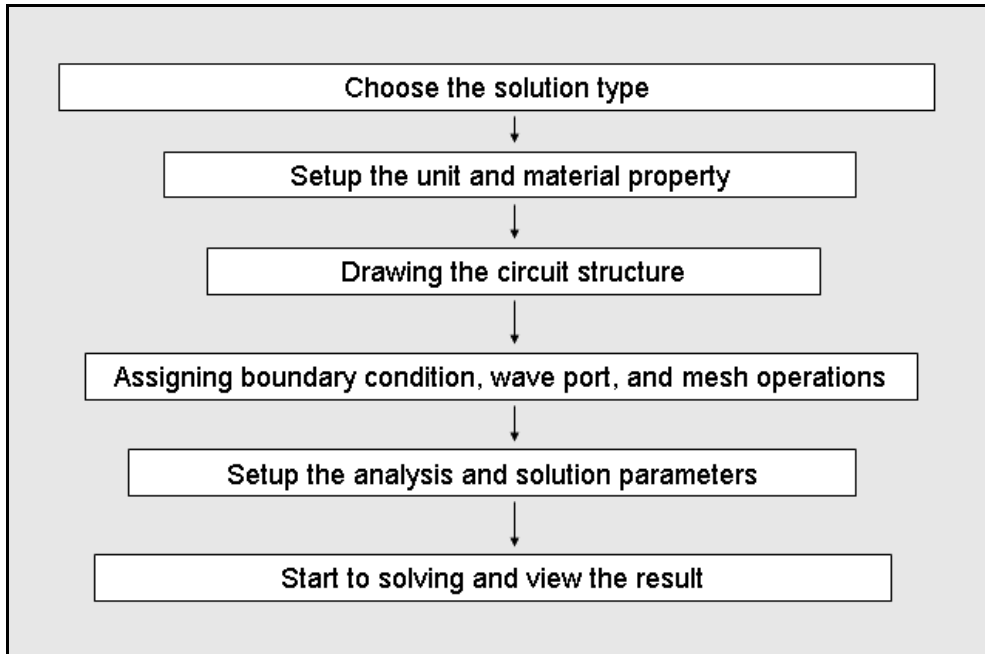


Fig. 3-1 The Ansoft HFSS simulation procedures

3.1.2 ANSYS

ANSYS is a general tool used finite element method (FEM) to simulate dynamics, thermal, and electromagnetic problems. In this section, it will be simulated Si_3N_4 and copper bimorph actuator. The meshed model is electro/thermal element, element type SOLID 98. With the environment changing, the mechanical deformation and temperature will be calculated. Table 3-1 shows the detail material parameters in this simulation.

At 0.1 V, the temperature of the suspended inductor is shown in Fig. 3-2. It is from room temperature 25°C to 208°C . The highest displacement of the inductor is about $130\ \mu\text{m}$, as shown in Fig. 3-3. The location of the highest temperature and displacement is occurred at the end of loop. In this simulation, an important thing is known that the inductor should etch a cave about $100\ \mu\text{m}$.

Table 3-1 The material parameters in ANSYS simulation

	Si3N4	Cu
Young's Modulus(Pa)	270E9	130E9
Poisson ratio	0.27	0.34
Thermal Expansion Coef. (/K)	1.6E-6	16.5E-6
Thermal Conductivity (W/m-K)	2	401
Resistivity (Ω-m)	1E14	1.7E-8

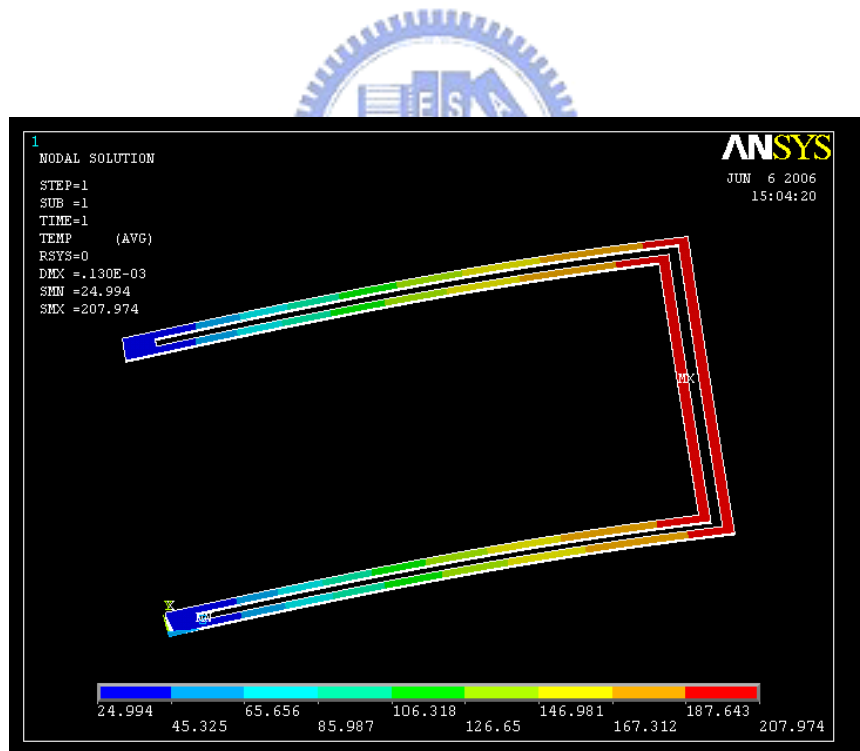


Fig. 3-2 The ANSYS simulation in temperature

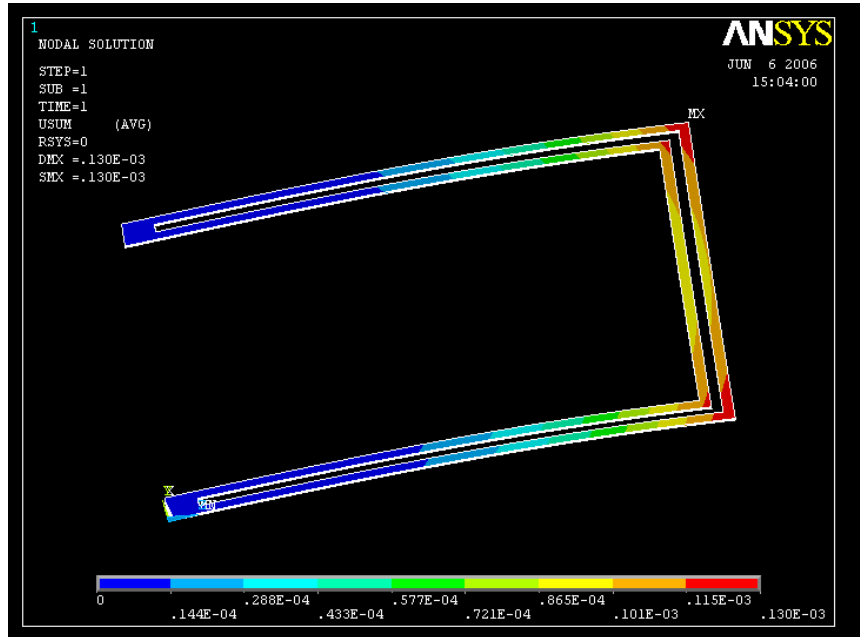


Fig. 3-3 The ANSYS simulation in displacement

3.2 Planar Circuit Design

It has been introduced the simulation procedures in last section. In this section, the detail RF inductor model will be described. Fig. 3-2 is the model which is established by HFSS. It has several parts in the model, including air box, substrate, isolation layer, circuit layout, and the port defined as input and output. Before simulation, the size of the inductor must be defined, as shown in Fig. 3-3. There are some parameters of the RF tunable inductor in this research as follows :

1. *Geometry* : It is used two-loop inductor and the outer loop is fixed by silicon nitride.
2. *Gap* : It means the distance between outer loop and inner loop. It is in place of G in the simulation..
3. *Width* : It means the width of the inductor metal, assumed the width is equal in each loop. It is in place of W in the simulation.
4. *Thickness* : It means the thickness of the metal in type A and type B inductors.

At the same time, the thickness of the silicon nitride is $0.6\mu\text{m}$.

5. *Material* : It means the composite of the inductor,

6. *The number of loop* : In this research, it has two loops.

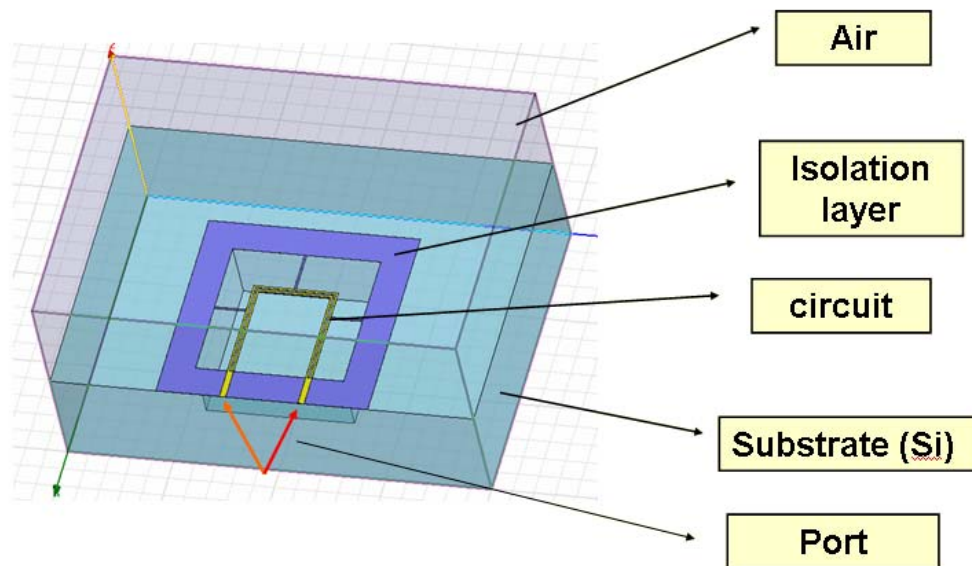


Fig. 3-2 The inductor model established by HFSS

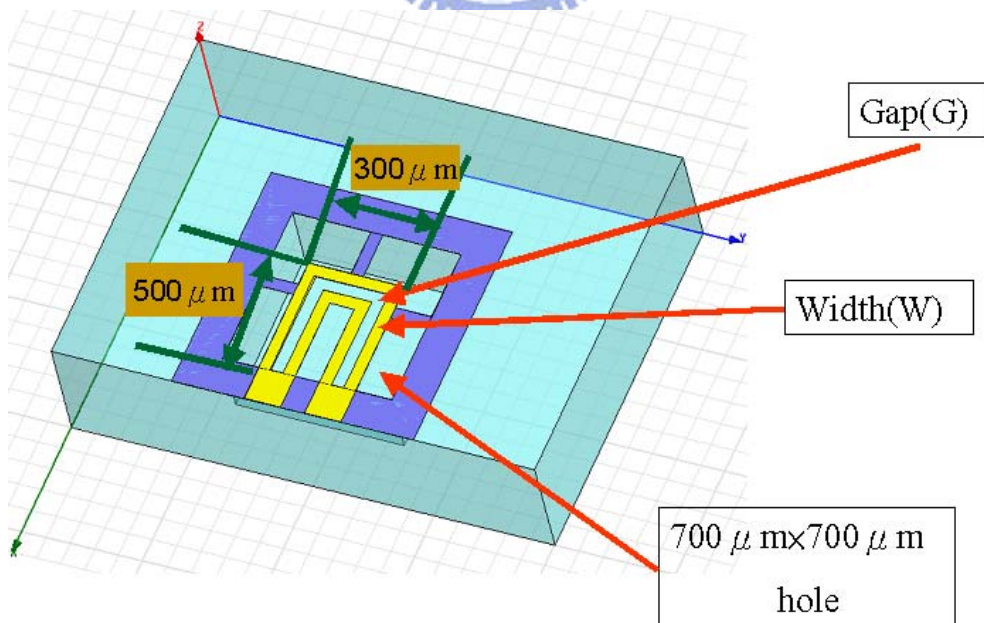
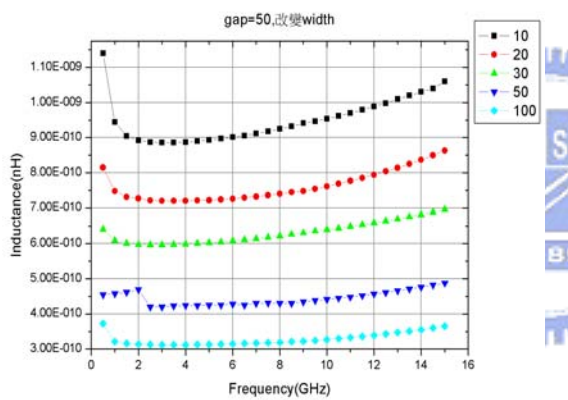


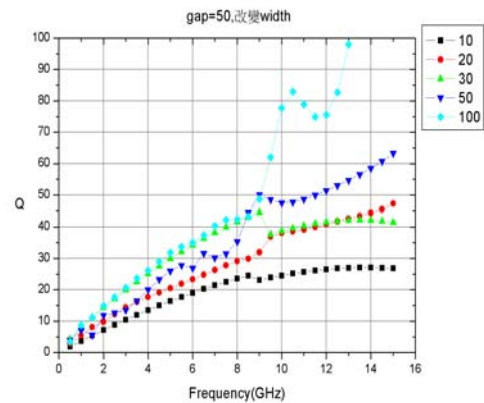
Fig. 3-3 The parameters of the RF tunable inductor

3.3 The Effects of Width and the Gap on the Inductors

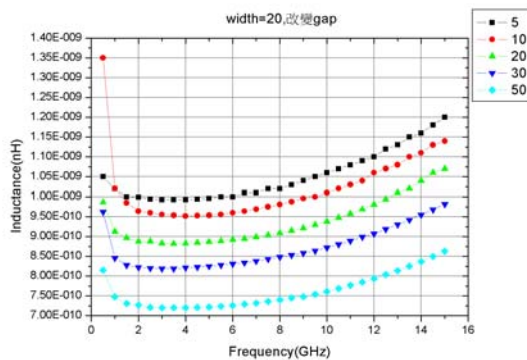
In this section, the influence of width and gap will be understood by simulation. First the effect of the width will be considered while other parameters are fixed. In this simulation, gap is $50\mu\text{m}$, the thickness of the metal, copper, is $1\mu\text{m}$, and the width is 10, 20, 30, 50, $100\mu\text{m}$. Second, this research will discuss the gap effect as the width is $20\mu\text{m}$. Last, integrating the width and gap will obtain what size is better for inductance and quality factor. These simulation results are shown in Fig 3-4.



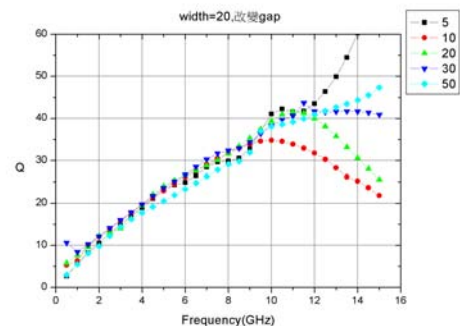
(a) W vs. L



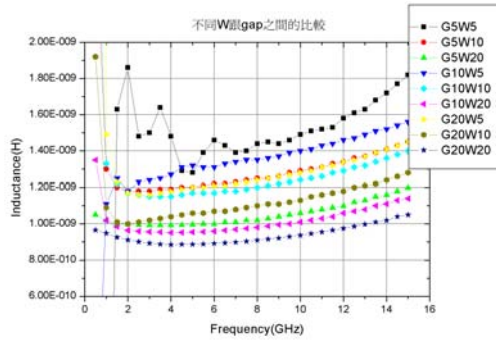
(b) W vs. Q



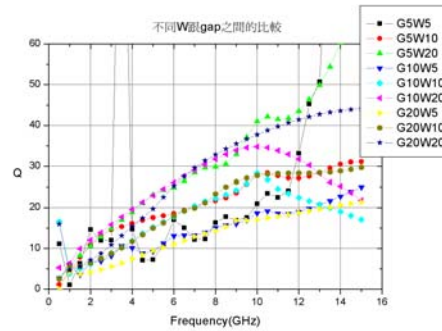
(c) G vs. L



(d) G vs. Q



(e) W and G vs. L



(e) W and G vs. Q

Fig. 3-4 The inductance and quality factor simulated by HFSS

In Fig. 3-4 (a) and (b), the inductance has the inverse ratio to the width and the quality factor has the direct ratio to the width. In Fig. 3-4 (c) and (d), the inductance has the direct ratio to the width and the quality factor has the inverse ratio to the width. It is important how to choose the suitable width and gap that keep the inductance and the quality factor high at the same time. It can realize what choice is better by observation Fig. (e) and (f).

In this research, the inductance and quality factor are better if they are higher. So there is a standard that the inductance is higher than 1 nH and the quality factor is higher than 20 at 8 GHz. As a result, there are four types of size to be designed, such as G5W10, G10W10, G20W10, and G5W20. In order to draw the mask to be more convenient, G5W20 will be not considered.

3.4 The Effects of the Thickness of the Metal on Inductance and Q

In this section, the metal thickness will be considered. The effect of thickness on the inductance will be shown in Fig. 3-5. The effect of thickness on the quality factor will be shown in Fig. 3-6.

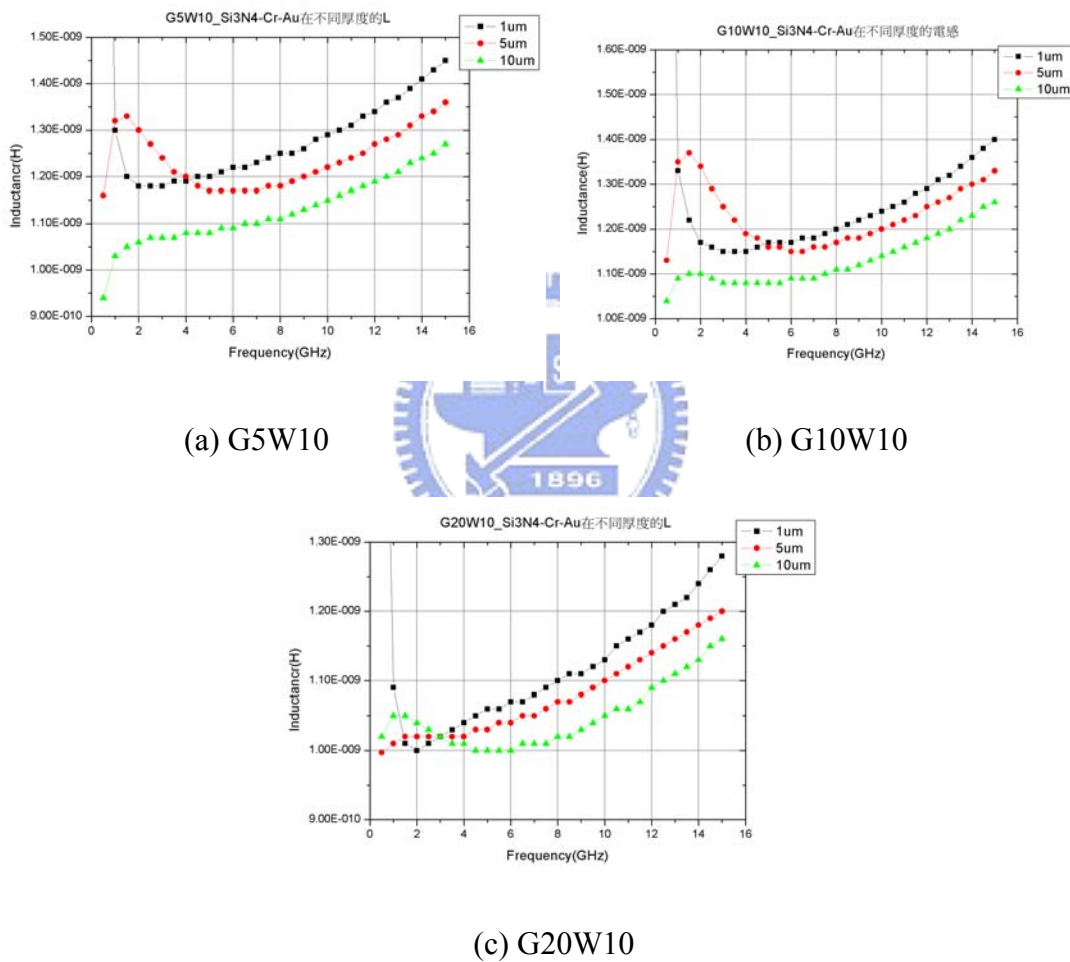
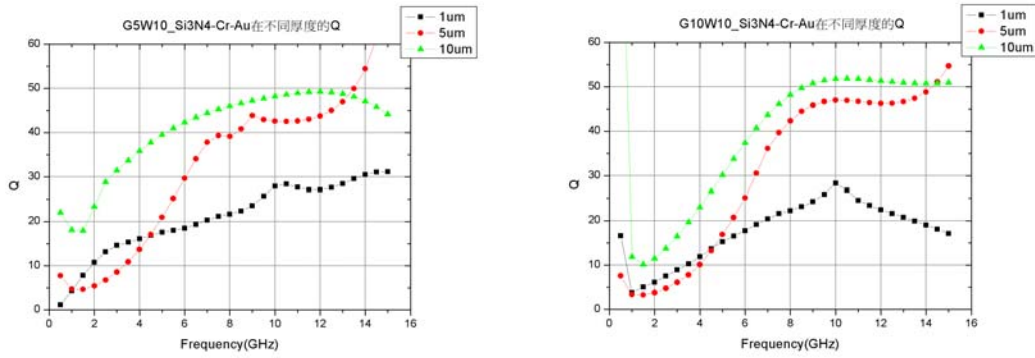


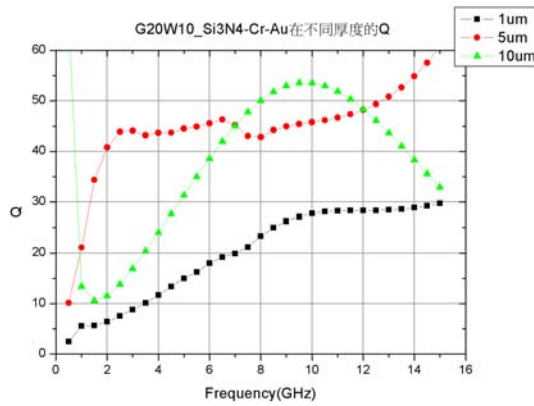
Fig. 3-5 The effect of thickness on the inductance

From Fig. 3-5, as the thickness is higher, the inductance will be less. By the way, the effect of thickness on the inductance is not so obvious.



(a) G5W10

(b) G10W10



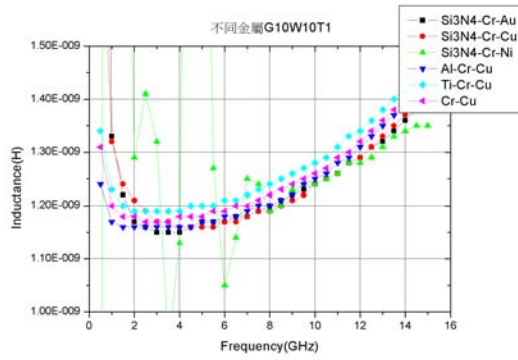
(c) G20W10

Fig. 3-6 The effect of thickness on the quality factor

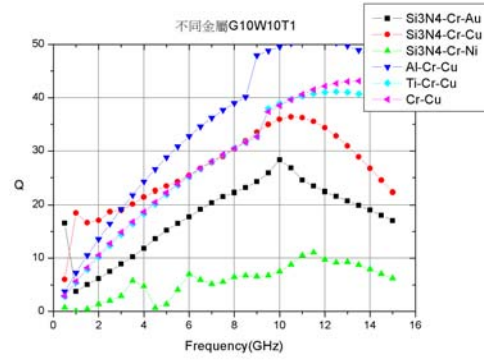
From Fig. 3-6, as the thickness is higher, the inductance will be higher. When the frequency is up to 15 GHz, the highest quality factor is the one whose thickness is 1 μ m.

3.5 The Effects of the Metal Materials on Inductance and Q

When the detail size inductor is designed, next step will be determined what materials should be used. In this simulation, the materials of the bimorph inductors will be Si₃N₄-Au, Si₃N₄-Cu, Si₃N₄-Ni, Al-Cu, Ti-Cu, and Cr-Cu. Their inductance and quality factor in simulations are shown in Fig. 3-7.



(a) Inductance



(b) Quality factors

Fig. 3-7 Effects of Different materials on the simulated inductance and quality factor

It is the preliminary simulation because it is based on the fabrication ability in the laboratory. After fabricating these inductors and measurement, the result will be compared to the ones simulated in order to make sure the trend if match each other.



Chapter 4 Fabrication Process

Traditional MEMS technology is defining the pattern by deposition, exposure, development, and etching on silicon wafer. In general, MEMS fabrication technology can be divided into three parts, surface micromachining, bulk micromachining, and LIGA technology.

The surface micromachining technology is evolved from integrated circuit technology. The structure is fabricated in bottom-up by lithography, etching and remove the sacrificial layers to construct the structure.

The bulk micromachining process is a top-down method. It can be defined a huge volume to use this technology. It uses the different etching rate in each Si direction to construct the structure.

LIGA technology uses the X-ray of synchrotron radiation as the exposure light source. It can fabricate a high aspect ratio structures.

In this chapter, the inductor fabrication will be illustrated and described, including lithography, etching, sputtering, and electroplating.

4.1 Fabrication Flowcharts of Three Types Inductors

There are three types of RF tunable inductors in this research. The fabrication process is involved lithography, sputtering, electroplating, and etching. Three of them will be introduced in detail. Table 4-1, 4-2, and 4-3 demonstrate the fabrication processes and the isotropic and cross-section view.

Table 4-1 Fabrication flowcharts of type 0 inductor

Process	3-D and cross-section view (not to scale)	
(1) Sputter Ti, Cu and Lithography		<p data-bbox="997 533 1316 616"> ■ PR ■ Cu ■ Si₃N₄ ■ Ti ■ Si </p>
(2) Electroplating		
(3) Remove photoresist, Cu, and Ti		

Table 4-2 Fabrication flowcharts of type A inductor

Process	3-D and cross-section view (not to scale)	
(1) Lithography		<p data-bbox="1077 1691 1252 1780"> ■ PR ■ Si₃N₄ ■ Si </p>
(2) RIE etching		





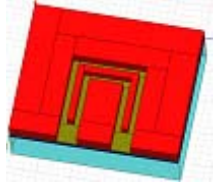
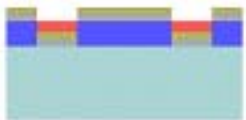
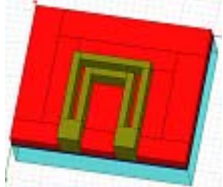
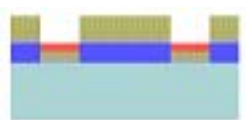
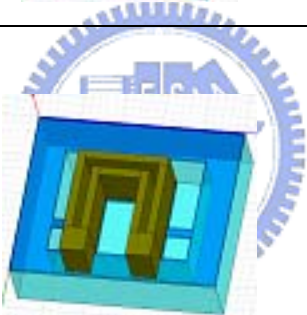





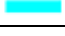
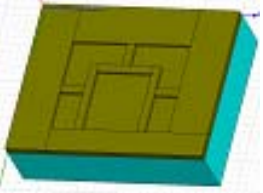
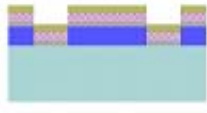
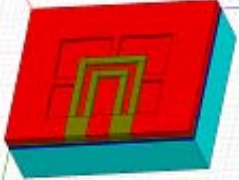


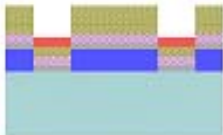
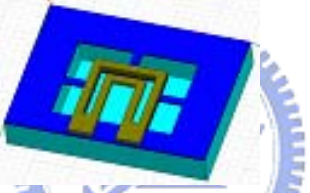
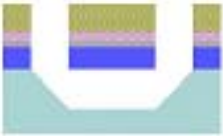
<p>(3) Remove the photoresist and Sputter Ti, Cu</p>		 <p>  Cu  Ti </p>
<p>(4) Lithography</p>		
<p>(5) Electroplating</p>		
<p>(6) Remove photoresist, Cu, and Ti (7) XeF2 dry etching and KOH etching</p>		

Table 4-3 Fabrication flowcharts of type B inductor

Process	3-D and cross-section view (not to scale)	
<p>(1) Lithography (2) RIE etching</p>		 <p>  PR  Si₃N₄  Si </p>

<p>(3) Remove the photoresist and sputter metal#1, Ti, Cu</p>		 <p> Cu Metal1 Ti </p>
<p>(4) Lithography</p>		
<p>(5) Electroplating</p>		
<p>(6) Remove photoresist, Cu, metal#1 and Ti (7) KOH etching</p>		

4.2 Substrate Selection and Clean

The inductor will warp when the temperature rising. Therefore, in order to have a space for the inductor to curve, the substrate has to be removed. Besides, it can increase the quality factor to remove the substrate so that the inductor and the substrate will be far away. Therefore, in this thesis, the Si is the choice to be the substrate of the inductors.

4.3 Lithography

In this process, AZ-P9260 is chosen to be defined the pattern in order to remove the silicon nitride and for the Cu electroplating mold. In this research, the photoresist will be spun 5 μm thickness.

4.4 Reactive Ion Etching

Because some parts of the silicon nitride must be etched, the Reactive Ion Etching, RIE, will be used in this process. The step is fabricated by National Chiao-Tung University Nano Facility Center (Semiconductor Research Center). After this process, the isolation layer photoresist will be removed by using sulfuric acid and hydrogen peroxide mixed liquid.



4.5 Sputtering

The materials of the inductors have several metals, such as Cu, Ti, Al, Ni, and Cr. The copper is usually deposited by electroplating. Before that, the adhesion layer and seed layer must be sputtered. The function of the adhesion layer is add the adhesion force of silicon nitride and the copper. The seed layer will promote the electroplating ability and performance. Besides, the metal which is one of material in the inductor structures can be also sputtered. The adhesion layer is usually about 100~300 \AA and the seed layer is about 1000~3000 \AA . The constitution of titanium and copper is the most suitable selection for copper electroplating.

4.6 Electroplating

After sputtering the adhesion layer and the seed layer, the structure of the inductor will be electroplated in the metal copper. It is convenient to fabricate the inductor by electroplating copper because it can vary the thickness by controlling the time and the current density. If the current density is too low, the structure will become rough and rugged. On the other hand, if the current density is too high, the structure will be warped or suspended. The current density is set and controlled around 0.07 to 0.1 ASD. [13] In this thesis, 1 μ m thick copper will be electroplated.

4.7 Dry and Wet Etching

The copper and titanium except the device must to be removed and isolated each independent device to measure the high frequency characteristics. It would be the ammonia water and hydrogen peroxide mixed liquid to etch copper. In addition, the BOE and the DI water mixed liquid will etch the metal titanium.

At last, in order to keep a space which the inductor can warp in, the substrate will be removed as a deep hole. In this research, the KOH etching method is used because it is anisotropic etching so that the substrate under the inductor can be removed clearly.

However, because of the geometry of the inductors, some place can not be etched very clean, as shown in Fig.4-1 (a). But if the inductor is used to XeF₂ Si isotropic etch first, as shown in Fig. 4-1 (b), then use KOH etching. In this way, the inductor will be suspended so that the inner loop of the inductor can be tuned, as shown in Fig. 4-1 (c).

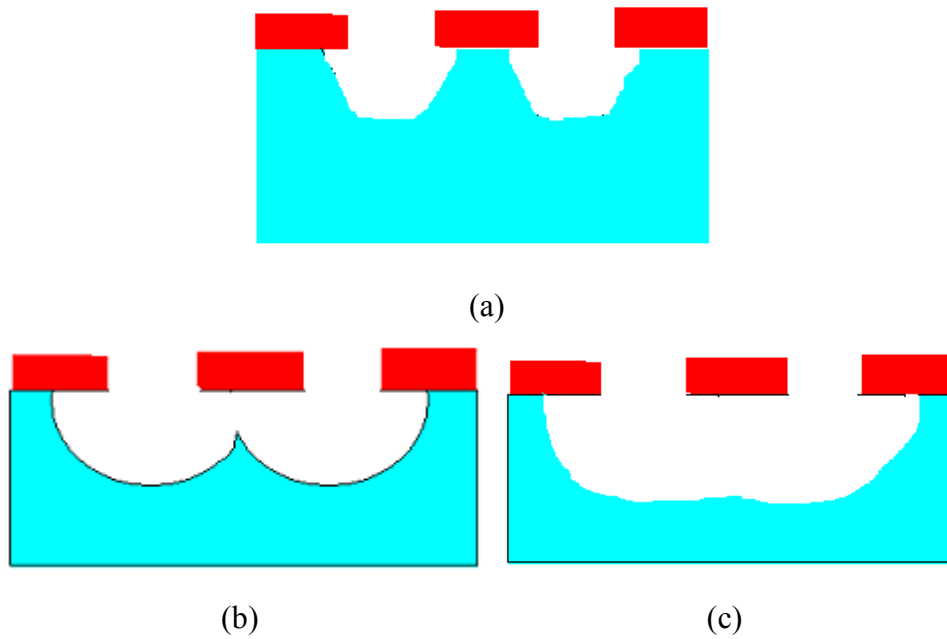


Fig. 4-1 The sketch map of etching substrate (a) only KOH etching
 (b) XeF2 etching first (c) after XeF2 and KOH etching

4.8 Fabrication Results

In section 2-10, three types inductors are mentioned. Type 0 and type A have been fabricated. Type B is failed because the metal Al will be etched by KOH and the metal Ti and Cr which are deposited by sputter have crevice.

Fig. 4-2 is the overview of type 0 inductors. Fig. 4-3 (a) is the SEM image of type A whose size is G20W10, and Fig. 4-3 (b) is its over view including a open circuit.

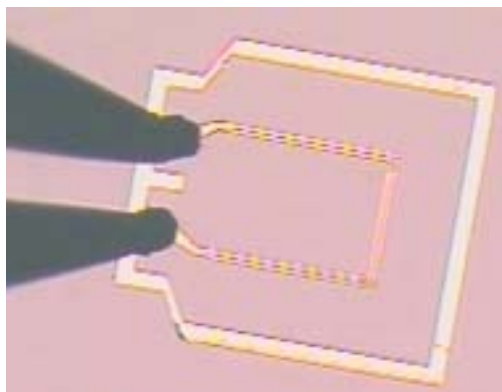


Fig. 4-2 The overview of type 0 inductors

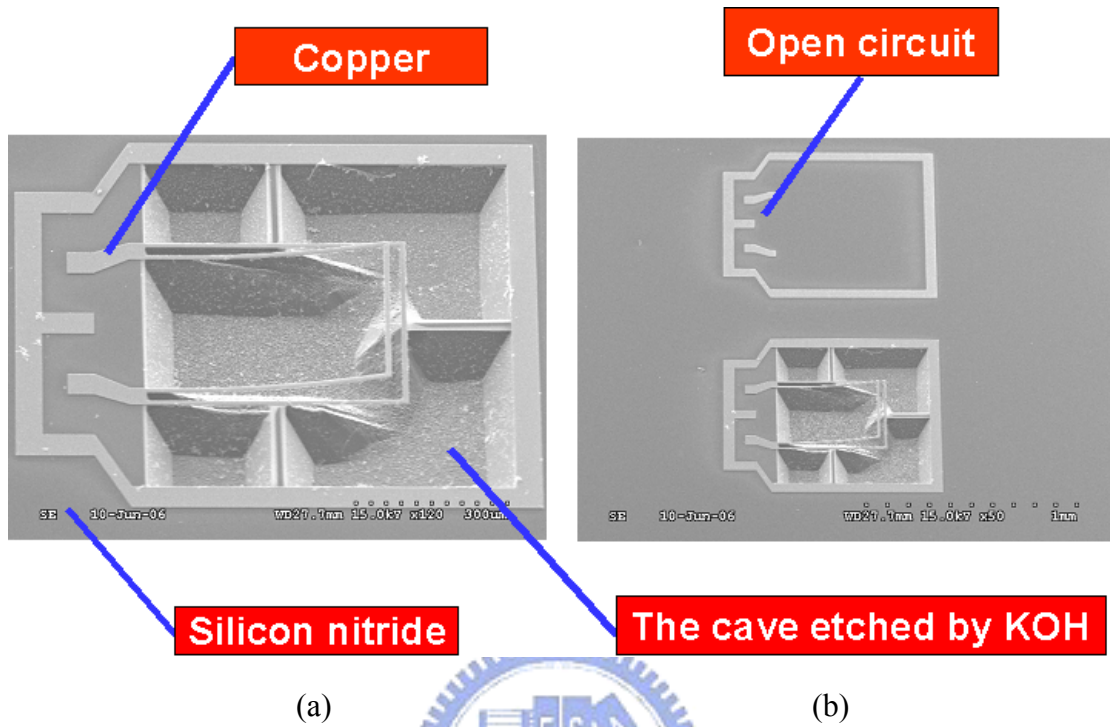


Fig. 4-3 The SEM image of (a) type A G20W10 inductor (b) type A G20W10 inductor and its open circuit

4.9 Mask Layout

The mask layout is shown in Fig. 4-4. Because of the measurement rule in NDL, in addition to the inductor itself, the layout must be drawn the metal loop as the ground line. The words G, and S in Fig. 4-4 mean the ground line and the signal line. Therefore, the probes can measure the high frequency characteristics.

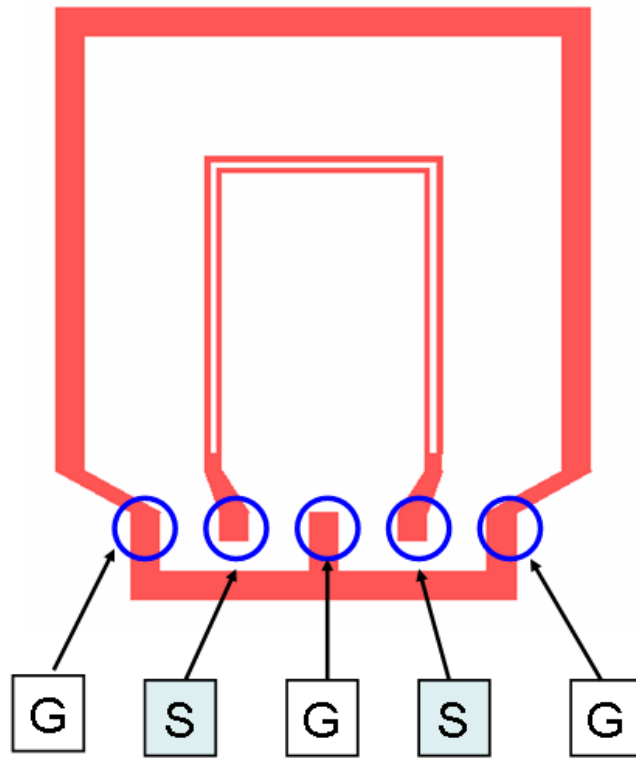


Fig. 4-4 The mask layout of the tunable inductor



Chapter 5 Measurement and Result

The S-parameters of the inductors in this thesis can be measured. The inductance and quality factor will be calculated by the S-parameters. In order to facilitate the measurement to obtain the S-parameters of the inductors, the extra test pad has to be incorporated in the structure of the device. At high frequency, those structures will generate extra influence on the measured data. In order to obtain the real S-parameters or inductance of the inductor, the additional effect has to be eliminated. Therefore, the inductor must to be de-embedded the extra parasitic effect which comes from the pad, an open pattern circuit of pads, grounded metal without two loops inductors fabricated with the inductors.

5.1 De-embedded Procedure of Measurement

As the Fig. 5-1(a), it is the layout (DUT) of an inductor, including the inductor and the GSGSG pad. So the S-parameters measured by the network analyzer contain not only the effect of the inductor but also the parasitic effect of the GSGSG (Ground, Signal, Ground, Signal, Ground) pad. In order to eliminate the effect of the pad, the GSGSG pad (Dummy) without two loops inductor is fabricated, as Fig. 5-1(b).

While the DUT is measured, the dummy will also be measured at the same time. Next transport the S-parameters of DUT and dummy to Y-parameters. The Y-parameters of DUT substrate the one of dummy is the Y-parameters of the inductor as the equation 5-1 :

$$Y_{inductor} = Y_{DUT} - Y_{dummy} \quad (5-1)$$

From a well-known property of transmission line, a section of transmission lines with the length l , the characteristic impedance Z_0 , the complex propagation constant γ . The series inductance can be obtained in equation 5-2 : [16]

$$L_s = \frac{im(\gamma \cdot l \cdot Z_0)}{2 \cdot \pi \cdot f} \quad (5-2)$$

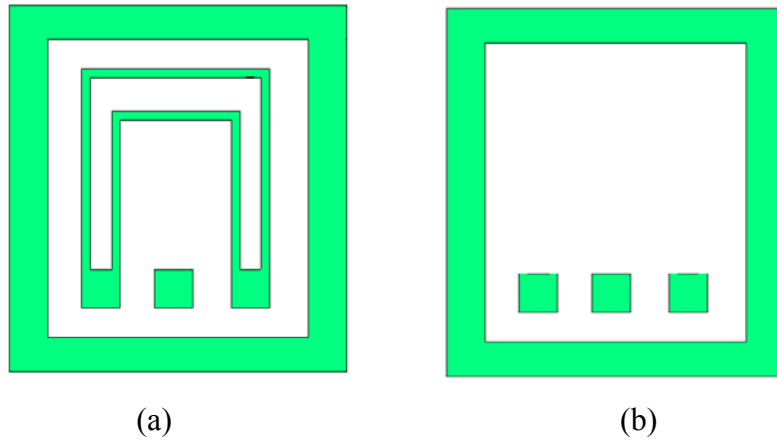


Fig. 5-1 The sketch of (a) DUT (b) Dummy

5.2 On Wafer Measurement

S-parameters measured by network analyzer E8364B and microprobes are shown in this section. The outline diagram of 4-port S-parameter Measurement System setup in NDL (Nano Device Laboratory) is shown in Fig. 5-2.

The operating frequency in this thesis is from 0.5~40 GHz, using GSGSG probe, and the minimum area of pad is $50\mu\text{m} \times 50\mu\text{m}$, the pitch of ground and signal $150\mu\text{m}$. Before measuring the parameter, the network analyzer must to be calibration, using SOLT (Short, Open, Load, Thru) calibration kits to define the SOLT reference plane.

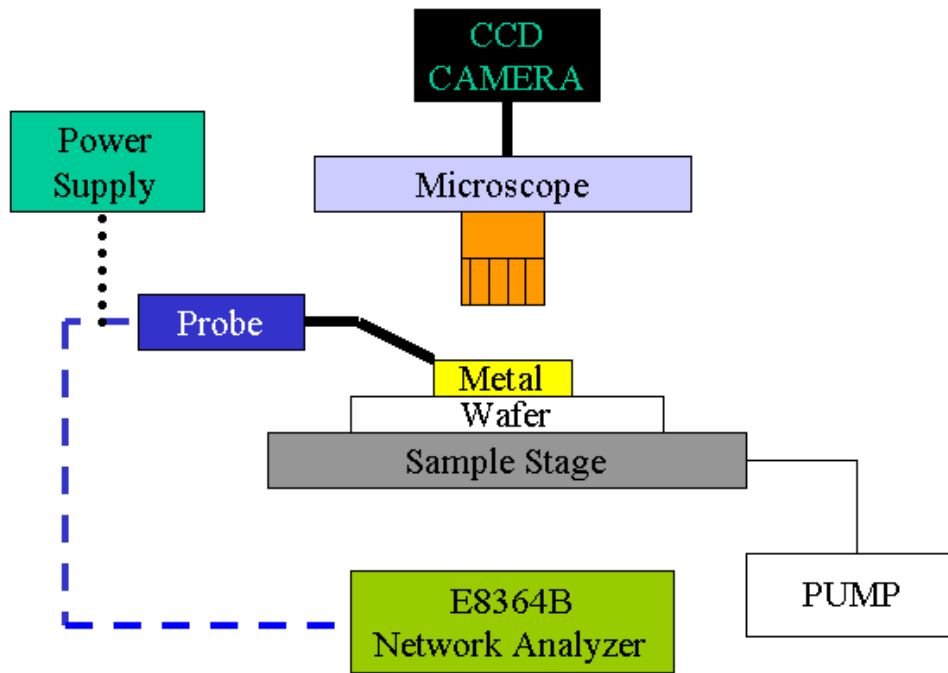
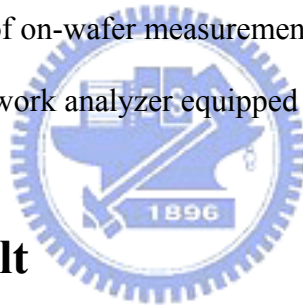


Fig. 5-2 The outline diagram of on-wafer measurement setup with microprobes station and vector network analyzer equipped in NDL RF Lab.



5.3 Measured Result

This section will introduce the measured result of type 0 and type A inductors. It contains the inductance and quality factor of type A before tuning and their tuning range. The comparison of inductance, quality factor between measurements and simulations by HFSS will also be mentioned. In the end, the quality factor of type 0 and type A will be discussed.

5.3.1 Measured Inductance before Tuning

Fig. 5-3 shows the measured inductance before tuning of type A. The inductance is from 1 nH to 2 nH. As the gap increases, the inductance will decrease. The measured results show that their operating frequency is all over 30GHz.

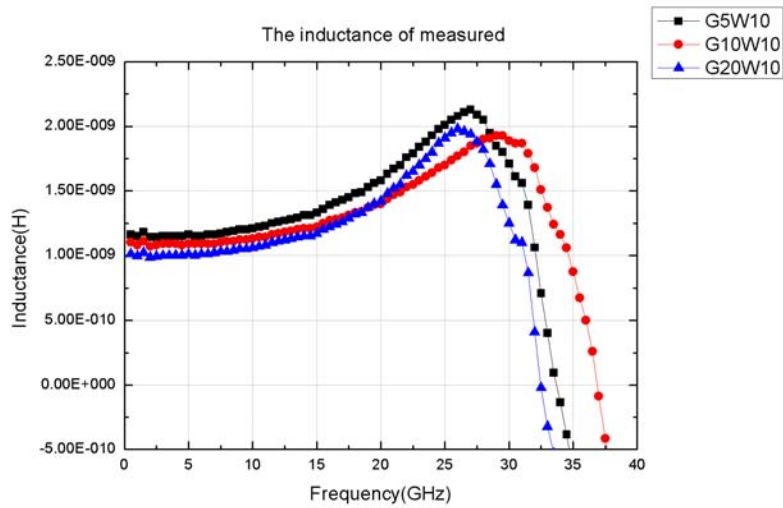


Fig. 5-3 The measured inductance before tuning

5.3.2 Measured Quality Factor before Tuning

Fig. 5-4 shows the measured quality factor before tuning of type A. The highest quality factor is 16.8. The measured results all show that their operating frequency is also over 30GHz. It can be understood that the gap of the inductors doesn't play an important role in quality factor improvement.

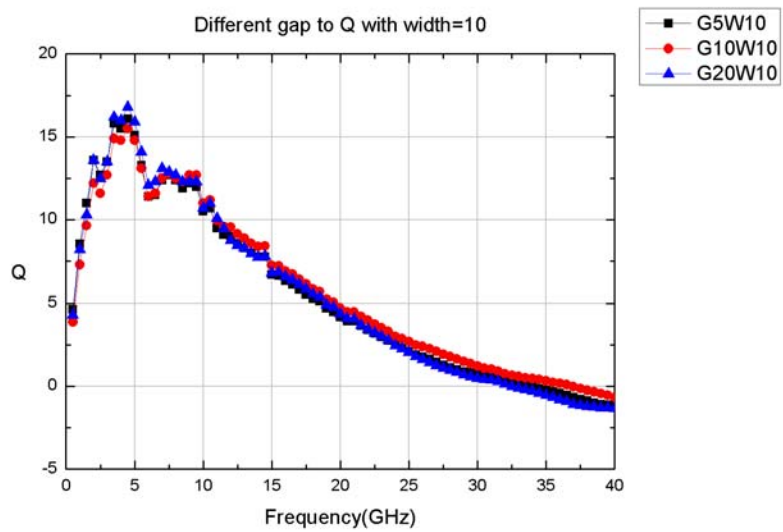


Fig. 5-4 The measured quality factor before tuning

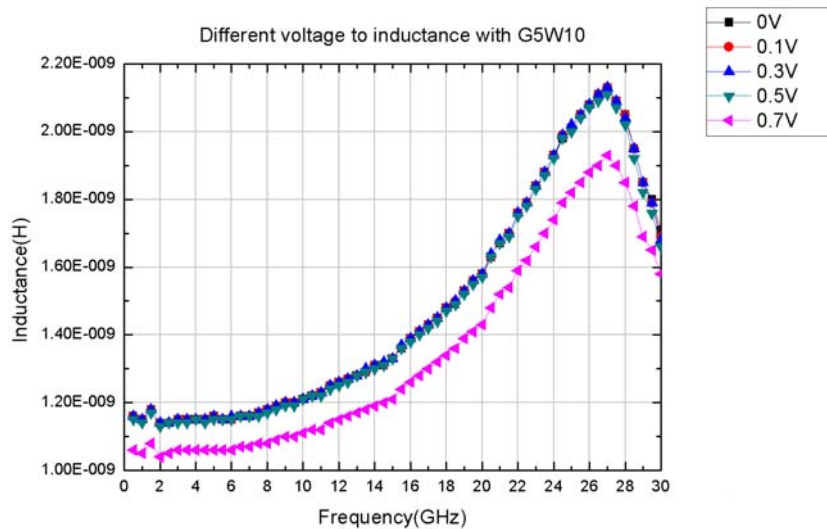
5.3.3 The Inductance Tuning

In chapter 3, the ANSYS simulation results have shown that the temperature and displacement will rise while inputting voltage. From section 2-10, while the temperature is increasing, the outer loop and inner loop will be winded because of the difference of the thermal expansion. Therefore, the inductance will be tunable.

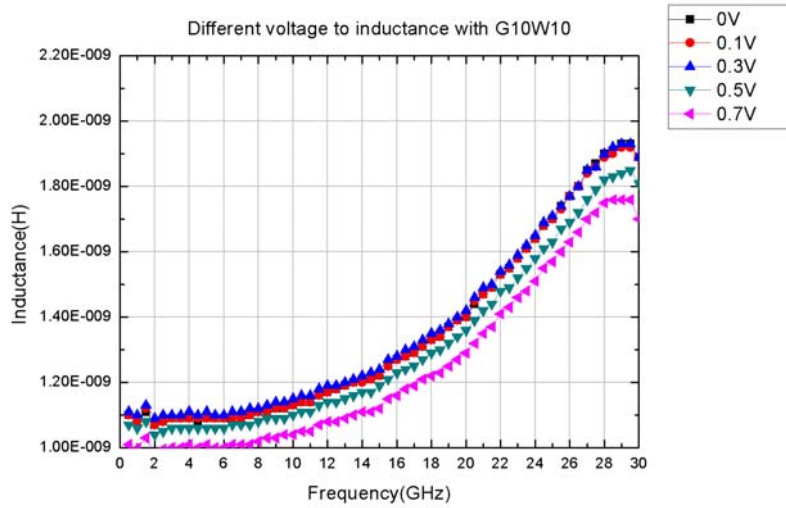
The input voltages on the tunable inductors in this thesis are 0V, 0.1V, 0.3V, 0.5V, and 0.7V. Fig. 5-5 shows the inductance tuning range of type A. The variation of the inductance ΔL can be shown in equation 5-1 :

$$\Delta L = \frac{L_{\max} - L_{\min}}{L_{\min}} \times 100\% \quad (5-1)$$

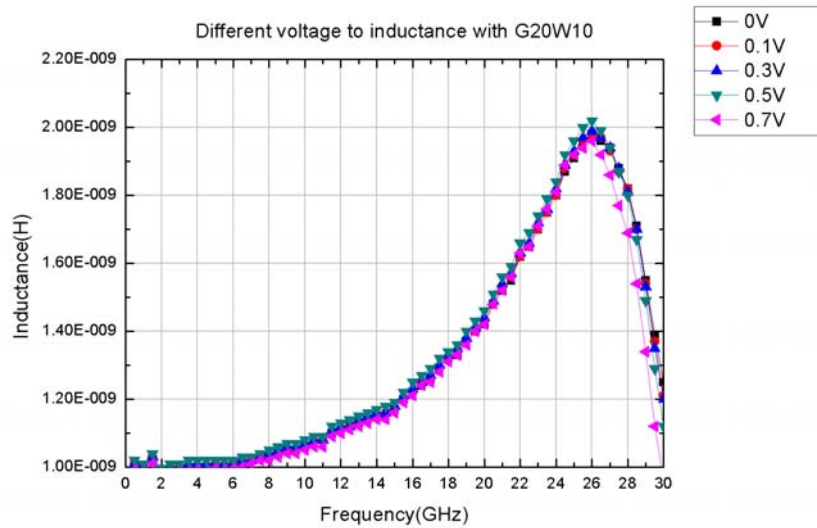
In G5W10, the difference of inductance from 0V to 0.7V for the maximum inductance is 1.93nH~2.13nH, $\Delta L=10.4\%$. The tuning inductance of G10W10 is 1.76nH~1.93nH, $\Delta L=9.7\%$. The tuning inductance of G20W10 is 1.92nH~1.96nH, $\Delta L=2.1\%$.



(a)



(b)



(c)

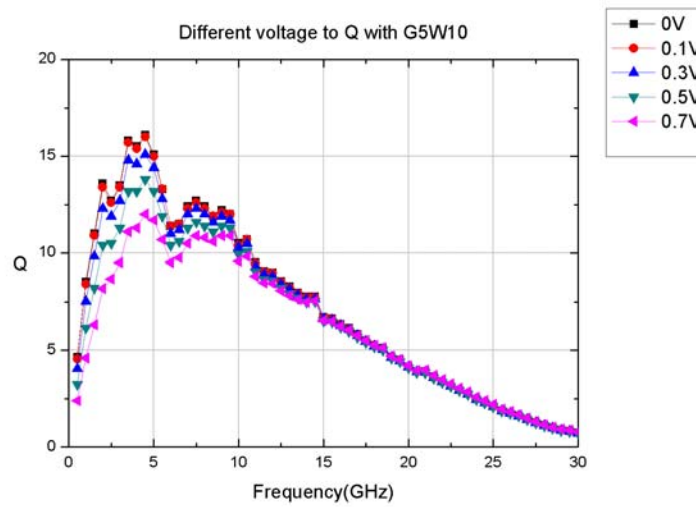
Fig. 5-5 The measured inductance tuning in (a) G5W10 (b)G10W10 (c) G20W20

5.3.4 The Quality Factor Change with Tuning

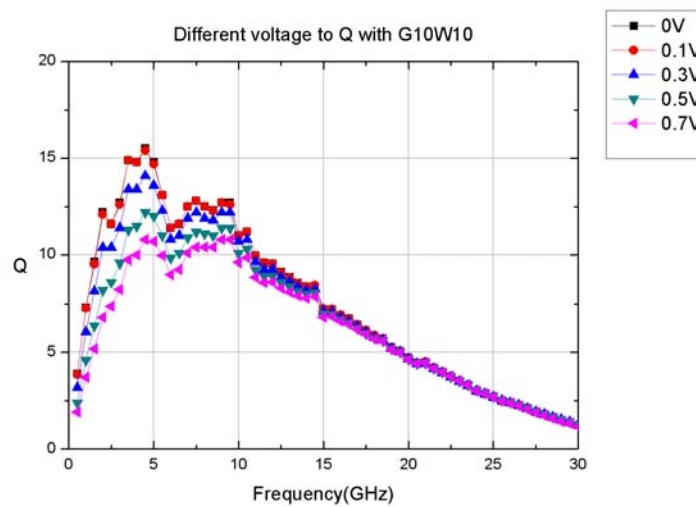
The purpose in this section is to discover the quality factor change range with tuning. Because the heat affects the magnetic wave transport, the quality factor will decrease.

However, the quality factor of the tunable inductors should be changed least. In this way, the tunable inductors would be reliable. Fig. 5-6 shows the measured quality factor change with tuning in (a) G5W10 (b) G10W10 (c) G20W20.

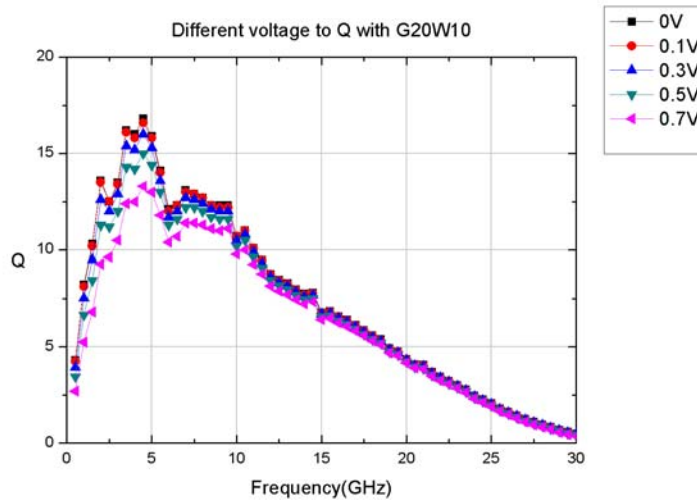
All the quality factor in these tunable inductors are about 12~17 with the inductors tuning. The quality factor change is not so large, so the inductors in the thesis can conform to the expectation from this measurement.



(a)



(b)



(c)

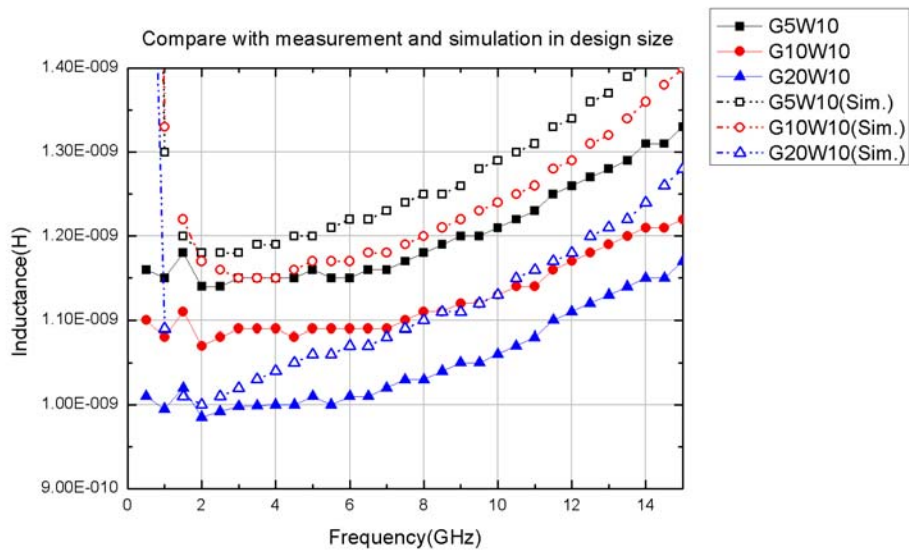
Fig. 5-6 The measured quality factor change with tuning in (a) G5W10 (b) G10W10
(c) G20W20

5.3.5 Comparison between Measurements and Simulations

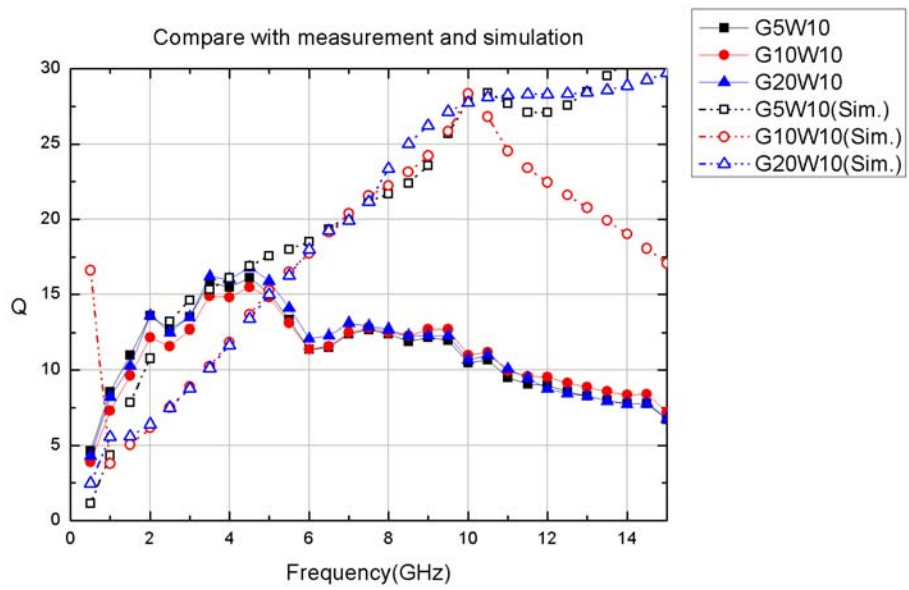
Fig.5-7 (a) and (b) show the comparison between measurements and simulations in inductance and quality factor of type A. In designed dimension, the gap(G) is 5, 10, and 20 μm , the width(W) is 10 μm . However, the real size of the inductors is not the same as the designed size. After the lithography process, the dimension of G5W10 will become G7W8, G10W10 to G9W10, G20W10 to G22W8. Besides, the copper electroplated after dry and wet etching will change its characteristic.

At 8GHz, the measured inductance of G5W10 is 1.17 and simulation result is 1.25. G10W10 is from 1.1 to 1.2; G20W10 is from 1.02 to 1.1. The distance of inaccuracy between measurement and simulation is only 0.1nH.

The quality factor is 27 from simulation, and it is higher than 17 from measured. It is predictable because the quality factor will decrease in real case from the fabrication, air, temperature, light and other electromagnetic wave.



(a)



(b)

Fig. 5-7 Comparison measurements and simulations in (a) inductance and (b) quality factors

5.3.6 The Quality Factor of Type 0 and Type A

Type 0 inductors are non-tunable inductors without digging Si cavity. Type A inductors are tunable inductors dug an $100\ \mu\text{m}$ cavity by using XeF_2 Si isotropic etch and KOH anisotropic etch.

The comparison of quality factor between type 0 and type A is shown in Fig. 5-8. Before digging Si cavity, the quality factor of type 0 is only 5.35. After digging an $100\ \mu\text{m}$ cavity, the quality factor can be up to 16.8. The quality factor can be improved 214% indeed by etching an $100\ \mu\text{m}$ deep hole.

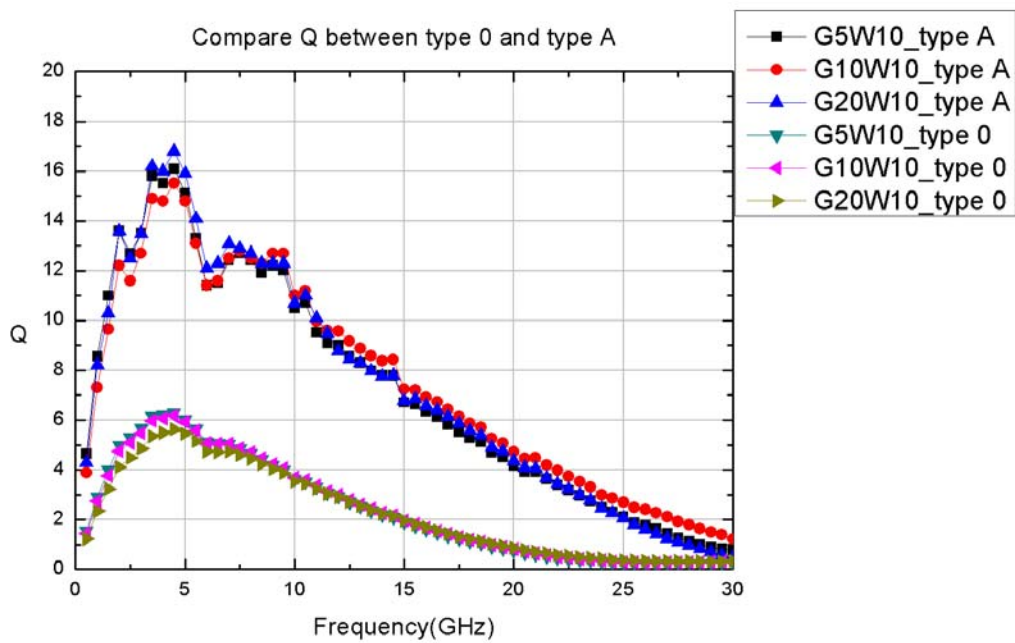


Fig. 5-8 The quality factor of type 0 and type A

Chapter 6 Summary and Future Work

6.1 Conclusions

Three types of inductors are designed by using two-loop bimorph actuators. Three RF tunable inductors have been designed with an electro-thermal bimorph actuator, and the inductance will be higher than 1 nH. The parameters, such as materials of the structure, width, gap, and the thickness, are considered to simulate the high frequency characteristics which includes inductance and quality factor. The inductance and Q simulated by HFSS are above 1 nH and 20 respectively. When the inductor has an input voltage the mutual inductance will change. Besides, the resonant frequency is above 15GHz by simulation. Furthermore, the full size of the inductor about $540\mu\text{m} \times 300\mu\text{m}$ is smaller than general ones.

Through HFSS simulation, a design process has been completed. Different kinds of metal materials in the inductor will be used and compare with the simulation. We also predict that while the increasing thickness can improve Q inductance will decrease not much. Besides, the inductance will increase with smaller gap between outer loop and inner loop and the gap won't influence the quality factor very much.

In ANSYS simulation, an important thing to know is that the inductor should etch a cave about $100\mu\text{m}$.

The silicon nitride is $0.6\mu\text{m}$, and the copper is about $1\mu\text{m}$ with the 300\AA titanium as an adhesion layer. Type 0 and type A inductors have been fabricated by using surface and bulk micromachining.

High frequency characteristics of the RF tunable inductors are measured with on-wafer measurement techniques by E8364B network analyzer at NDL RF-Lab.

All of the inductance is over 1nH. The resonant frequency is above 30GHz and the best quality factor is 16.8 at 5GHz. The inductance tuning range is up to 10.4%.

While the thermal deformation changes, the quality factor remained stable around 12 to 17. At last, the quality factor can be improve from 5.35 to 16.8 after etching 100 μ m deep cavity.

6.2 Future Work

In future, several suggestions are presented in order to have more complete and systematic research.

- (1) In order to increase the accuracy of simulation, the more dense mesh has to be applied in HFSS and the detail mechanical characteristics have to be investigated such as Young's Modulus, thermal expansion coefficient, thermal conductivity and resistivity.
- (2) Based on HFSS, the geometry and dimension can be continued improved and investigated by using the design process in this thesis.
- (3) Try to use other metal materials as the inductors and choose the suitable way to etch the substrate.

Reference

- [1] Hector J. De Los Santos , "RF MEMS Circuit Design for Wireless Communications" , 2002
- [2] 刑泰剛, 工研院材料所, 「MEMS 在無線通信應用發展趨勢」, 工業材料雜誌, 184 期, 91 年 4 月
- [3] 微機電系統技術與應用, 行政院國家科學委員會精密儀器發展中心出版
- [4] D.R. Pehlke, A. Burstein, M.F. Chang , "Extremely High-Q Tunable Inductor for Si-Based RF Integrated circuit applications" , IEDM,1997 IEEE
- [5] Shifang Zhou, Xi-Qing Sun, and William N. Carr , "A Micro Variable Inductor Chip Using MEMS Relays" , 1997 International Conference on Solid-State Sensors and Actuators
- [6] Victor M. Lubcke , Bradley Barber, Edward Chan, Daniel Lopez, Mihal E. Gross, and Peter Gammel , "Self-Assembling MEMS Variable and Fixed RF Inductors" , IEEE transactions on microwave theory and techniques, VOL. 49, NO. 11, November 2001
- [7] T. Fukushige, Y. Yokoyama, S. Hata, K. Masu, A. Shimokohbe , "Fabrication and evaluation of an on-chip micro variable inductor" , Microelectronic Engineering 67-68 (2003) 582-587
- [8] I. Zine-El-Abidine, M. Okoniewski and J.G, McRory , "A tunable RF MEMS Inductor" , 2004 International Conference on MEMS, NANO and Smart Systems
- [9] Imed Zine-El-Abidine, Michal Okoniewski and John G McRory , "Tunable radio frequency MEMS inductors with thermal bimorph actuators" , J. Micromech. Microeng. 15, 2005
- [10] Gabriel M. Rebeiz , "RF MEMS Theory, Design, and Technology"
- [11] Joseph F. White , "High Frequency Techniques" , WILEY-INTERSCIENCE

- [12] He'ctor J. De Los Santos , "RF MEMS Circuit Design for Wireless Communications" , Artech House
- [13] 余仁淵, "三維微小尺寸高頻微機電濾波器之設計、模擬與製作", 國立交通大學機械工程研究所碩士論文, 2003
- [14] Min Park, et al. , "The detailed analysis of high Q CMOS-compatible microwave spiral inductors in silicon technology" , IEEE Tran. On Electron Devices, Vol.45, No. 9, Sep. 1998
- [15] 簡業達, "微小化共面波導濾波器之設計、模擬與製作" , 國立交通大學機械工程研究所碩士論文, 2005
- [16] 林志瑋, "射頻微機電式電感器的最佳化設計" , 國立交通大學電子工程學系電子研究所碩士論文, 2004

